




Cite this: *Analyst*, 2024, **149**, 4135

## EXPAR for biosensing: recent developments and applications

Xinyi Ou, <sup>a,b</sup> Kunxiang Li,<sup>a,b</sup> Miao Liu,<sup>a</sup> Jiajun Song,<sup>a,b</sup> Zhihua Zuo\*<sup>c</sup> and Yongcan Guo\*<sup>a,b</sup>

Emerging as a promising novel amplification technique, the exponential amplification reaction (EXPAR) offers significant advantages due to its potent exponential amplification capability, straightforward reaction design, rapid reaction kinetics, and isothermal operation. The past few years have witnessed swift advancements and refinements in EXPAR-based technologies, with numerous high-performance biosensing systems documented. A deeper understanding of the EXPAR mechanism has facilitated the proposal of novel strategies to overcome limitations inherent to traditional EXPAR. Furthermore, the synergistic integration of EXPAR with diverse amplification methodologies, including the use of a CRISPR/Cas system, metal nanoparticles, aptamers, alternative isothermal amplification techniques, and enzymes, has significantly bolstered analytical efficacy, aiming to enhance specificity, sensitivity, and amplification efficiency. This comprehensive review presents a detailed exposition of the EXPAR mechanism and analyzes its primary challenges. Additionally, we summarize the latest research advancements in the biomedical field concerning the integration of EXPAR with diverse amplification technologies for sensing strategies. Finally, we discuss the challenges and future prospects of EXPAR technology in the realms of biosensing and clinical applications.

Received 24th April 2024,  
Accepted 9th July 2024

DOI: 10.1039/d4an00609g

[rsc.li/analyst](http://rsc.li/analyst)

### Introduction

It is well-established that the high sensitivity and specificity of clinical biomarkers not only play a crucial role in clarifying the molecular mechanism of diseases but also facilitate the selection of the most effective evidence-based treatment option after early detection to improve precision and individualized medicine.<sup>1–4</sup> However, these biomarkers are typically present in low quantities in biological specimens, especially during the early stages of the disease.<sup>5–7</sup> Therefore, the development of a sufficiently sensitive method for detecting these low-abundance expression level biomarkers is essential for the early diagnosis of diseases.

Nucleic acid-based signal amplification strategies are being widely employed for detecting pathogenic organisms and biological diseases. These techniques can be categorized based

on the temperature requirements during the reaction process. Thermal cycling amplification technologies, exemplified by the polymerase chain reaction (PCR), represent a conventional method for detecting extremely low concentrations of nucleic acids.<sup>8</sup> Isothermal amplification techniques (IATs), on the other hand, have emerged since the 1990s.<sup>9</sup>

The application of PCR in the field of rapid real-time diagnostics at point-of-care testing (POCT) is significantly limited by several factors. These include the requirement of expensive and complex thermal cycling equipment, the need for trained personnel, and extended reaction times. Additionally, non-specific primer annealing can produce false positive results, further hindering PCR's development in this context.<sup>10</sup> In comparison, IATs offer distinct advantages for nucleic acid-targeting and signal amplification. IATs boast streamlined experimental processes, high sensitivity, high inhibitor tolerance, and high fidelity.<sup>11</sup> Thus, IATs have emerged as a popular area of research for timely detection and POCT applications.

Isothermal amplification techniques can be categorized based on their reaction kinetics into linear amplification, cascade amplification, and exponential amplification. The latter category includes loop-mediated isothermal amplification (LAMP),<sup>12</sup> recombinase polymerase amplification (RPA),<sup>13</sup> helicase-dependent amplification (HDA),<sup>14</sup> nucleic acid sequence-based amplification (NASBA),<sup>15,16</sup> and exponential amplification reaction (EXPAR).<sup>17,18</sup> EXPAR technology utilizes

<sup>a</sup>Nanobiosensing and Microfluidic Point-of-Care Testing, Key Laboratory of Luzhou, Department of Clinical Laboratory, The Affiliated Traditional Chinese Medicine Hospital, Southwest Medical University, Luzhou, 646000, PR China.

E-mail: [guoyongcan@swmu.edu.cn](mailto:guoyongcan@swmu.edu.cn)

<sup>b</sup>Department of Laboratory Medicine, The Affiliated Hospital, Southwest Medical University, PR China

<sup>c</sup>Department of Clinical Laboratory, Nanchong Central Hospital, The Second Clinical Medical College of North Sichuan Medical College, Nanchong, Sichuan, 637003, PR China. E-mail: [zzhazard@163.com](mailto:zzhazard@163.com)



a single-stranded trigger probe (Trigger) X and a single-stranded functional template (Functional template) X'-X', where X' is complementary to Probe X. The two repeated segments of X' are connected by the cleavage site of a nicking endonuclease. This configuration enables EXPAR, under the combined action of the nicking endonuclease and a strand-displacement DNA polymerase, to amplify  $10^6$  to  $10^9$  fold within a short period (<30 minutes).<sup>19–22</sup> Notably, EXPAR shares similarities with the nicking enzyme amplification reaction (NEAR),<sup>17</sup> which can lead to confusion. Both EXPAR and NEAR employ a nicking endonuclease and a strand-displacement polymerase; however, NEAR utilizes a strand-displacement scheme, while EXPAR follows a linear amplification strategy.<sup>23</sup> EXPAR relies fundamentally on the transition from the thermal stability of double-stranded DNA to instability through the cleavage reaction, which severs phosphodiester bonds.<sup>24</sup> In conclusion, the EXPAR technique presents a promising and practical approach due to its isothermal nature, high amplification efficiency, broad dynamic range, rapid amplification kinetics, and straightforward design and operation procedures. It holds potential for applications in detecting a wide spectrum of small molecule biomarkers, including nucleic acids, DNA methylation patterns, proteins, enzymatic activities, and metal ion indicators.

At present, two main challenges exist for EXPAR technology: firstly, generating trigger DNA with a clear 3' end, which relies on fingerprint technology. However, this requires the use of different restriction enzymes for different target sequences, while also necessitating a head-to-head orientation of adjacent recognition sites in the double stranded DNA (dsDNA). In addition to the challenge of selecting appropriate endonucleases and reaction conditions for a given sequence, triggering DNA cleavage is only possible by dsDNA, with its 3' end located either within or near the recognition site. This greatly restricts the flexibility of EXPAR for detecting truly meaningful sequence fragments.<sup>25</sup> The second challenge concerns non-target amplification, encompassing early-phase non-specific background and non-template amplification.<sup>26,27</sup> The short length of the EXPAR template plays a critical role in triggering non-specific amplification during DNA polymerase catalysis.<sup>28,29</sup> These non-specific amplifications significantly hinder the detection of the target fragment, thereby limiting the applicability of EXPAR.

The robust application potential of EXPAR technology has driven many researchers to explore its integration with various biosensing methodologies. This strategy aims to overcome limitations inherent to conventional EXPAR formats and achieve enhanced amplification specificity, sensitivity, and overall efficacy. This review will critically analyze and discuss recent advancements in strategies that combine EXPAR technology with CRISPR systems, metal nanoparticles (MNPs), aptamers, alternative IATs, and nucleases. By delving into this broad landscape of EXPAR-based biosensing methodologies, we aim to provide novel research concepts and blueprint designs for realizing POCT and personalized precision medicine applications.

## The principle of EXPAR

EXPAR technology relies on several key components: triphosphate deoxyribonucleotides (dNTPs), template strands, DNA polymerase, and a nicking endonuclease (NEase). The amplification template plays a critical role in the EXPAR reaction. The standard template (X'-X' template) comprises two identical terminal fragments (X') with sequences complementary to the target sequence (X). These fragments are separated by a region recognized and cleaved by the NEase.<sup>30</sup> Upon introduction of the target sequence into the reaction system, it forms a heteroduplex with the 3' end region (X'(3'X'T)) of the template, acting as a primer for DNA polymerase to synthesize the complementary strand. This results in dsDNA containing the NEase recognition site in the middle. The NEase cleaves the extended dsDNA, generating gaps. DNA polymerase then extends the 3' end of the incision site and replaces the newly synthesized strand. Crucially, the template's two X' regions ensure that the replaced DNA strand has the same sequence as the trigger DNA. This replaced chain then hybridizes with another template strand, initiating a new amplification cycle. This process continues, amplifying the target DNA exponentially from the initial trigger-template complex. Consequently, each cycle generates two copies of triggering DNA from a single target molecule, achieving exponential amplification.<sup>31</sup>

## The optimization of the EXPAR template

A significant challenge associated with EXPAR technology is the high background phenomenon, primarily linked to high template concentration. This can lead to non-specific binding within the reaction system, including the formation of secondary structures within the EXPAR template itself, interactions between multiple template strands, and interactions between the template and other nucleic acids present in the sample.<sup>26,27,31</sup> To address this issue, previous studies have explored strategies to improve reaction specificity and reduce non-specific amplification in conventional EXPARs. These approaches involve chemical modification of the EXPAR template<sup>32–34</sup> or optimization of the template sequence design (Fig. 1).

Zou *et al.* introduced a novel isothermal amplification technique termed the symmetric exponential amplification reaction (SEXPAR) that utilizes structurally switchable symmetric toehold dumbbell-shaped templates (STD templates)<sup>35</sup> (Fig. 1E). The sealed and symmetrical structure of the STD template allows exponential amplification reactions to occur during each annealing cycle without compromising amplification efficiency. Additionally, the rigid and compact structure of the STD template, along with an appropriate standard free energy, ensures that SEXPAR is specifically activated only by the targeted miRNA. The results demonstrated that the SEXPAR method could detect let-7a at concentrations as low as 0.01 zmol with remarkably high specificity, effectively dis-



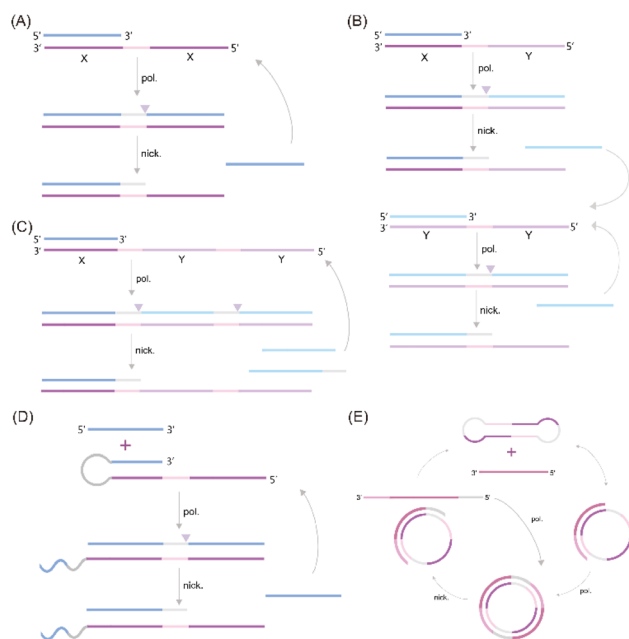


**Fig. 1** EXPAR-based microRNA detection. (A) Original EXPAR design using a single dual-repeat template (X–X, where X is the complementary sequence of the target miRNAs) comprising a nicking recognition site. The template catalyzes the exponential replication of the miRNA sequence through polymerization/nicking cycles.<sup>32</sup> (B) Similar strategies have been explored converting the target amplification to a signal amplification (where an arbitrary “Y” strand is amplified instead of the miRNA sequence itself) using an X–Y–Y template design.<sup>33</sup> (C) Two template designs X–Y and Y–Y.<sup>34</sup> (D) Strategies to enhance the target selectivity have been explored using a hairpin template design.<sup>30</sup> (E) Dumbbell template design.<sup>35</sup>

tinguishing even single-base mismatched miRNAs. Furthermore, the detection range was significantly extended to 10 orders of magnitude. These findings suggest that the SEXPAR method has the potential to serve as a powerful detection technology for miRNAs and other short nucleic acids. Building upon this research, the authors further combined SEXPAR with fluorescence *in situ* hybridization (FISH) in 2019, proposing the SEXPAR-FISH strategy.<sup>36</sup> This approach enables the imaging of intracellular specific miRNAs within cells. The detection range of SEXPAR-FISH spans from 1 fM to 10 nM, exhibiting superior sensitivity compared to those of traditional FISH techniques. It also facilitates faster quantitative visualization of trace amounts of miRNAs in cells compared to most FISH-based methods. Subsequently, they employed low-cytotoxicity lipid nanoparticles to encapsulate the SEXPAR components and deliver them into viable tumor cells, achieving sensitive and continuous imaging of intracellular miRNAs.<sup>37</sup>

Qu *et al.* introduced a novel and enhanced isothermal EXPAR technique termed circular EXPAR (cEXPAR), which utilizes a circular amplification template.<sup>38</sup> In contrast to linear templates, cEXPAR allows for random pairing of DNA or RNA fragments containing two repeated sequences. This design facilitates the rapid synthesis of short oligonucleotide fragments through concurrent incision and substitution processes.

Notably, cEXPAR exhibits high sensitivity, enabling the specific triggering of chain reactions from single-copy targets (1 ymol) and the discrimination of single nucleotide variations between miRNAs.<sup>38</sup> These capabilities suggest that cEXPAR detection holds promise as a valuable alternative method for rapid, sensitive, and highly specific miRNA detection.

Trinh *et al.* explored a strategy to reduce non-specific amplification in EXPAR by employing chemically modified cobalt hydroxide (CoOOH) nanosheets and hexanediol. The adsorption of these CoOOH nanosheets and the 3' end modification with hexanediol effectively prevent targetless polymerization of the template itself. This approach enables the detection of multiple miRNA targets at concentrations as low as 10 aM.<sup>39</sup> Notably, the strong adsorption and separation of nucleic acids by CoOOH nanosheets from complex sample matrices significantly reduce additional interference, particularly in serum samples. These findings suggest that this sensitive template-blocking EXPAR method has the potential to serve as a valuable approach for the discovery and verification of miRNA biomarkers in biological samples. Interestingly, Mao *et al.* proposed a novel self-passivating EXPAR template incorporating a thiophosphate ester modification.<sup>29</sup> This modification effectively inhibits non-specific interactions and prevents DNA polymerase from extending the template by thiophosphorylating template sequences prone to forming transient double-stranded DNA structures. This method exhibits a detection range of 1 fM to 1 nM, with a minimum limit of detection (LOD) of 0.7 fM. These improvements significantly enhance the applicability of classical EXPAR. Finally, Jiang *et al.* introduced polyethylene glycol 200 (PEG200) into the EXPAR system.<sup>40</sup> By acting as a co-solvent, PEG200 induces molecular crowding, which decreases the water activity within the solution. This, in turn, attenuates interactions between template strands and enzyme catalysis. This approach enhances the sensitivity of EXPAR by four orders of magnitude without extending analysis time, allowing for the detection of target miRNA at 1 aM within 20 minutes.

Lin *et al.* presented a novel strategy to enhance the specificity of EXPAR for miRNA detection. Their approach leverages the binding affinity of *Thermus thermophilus* Argonaute (TtAgo) to templates, enabling the effective elimination of non-specific hybridization between templates.<sup>41</sup> This TtAgo-mediated background suppression strategy achieved a detection limit of  $10^{-15}$  M, demonstrating a 1000-fold and 100-fold improvement in sensitivity compared to those of traditional RT-PCR and EXPAR, respectively. These findings suggest that protein enzymes, beyond their role in nucleic acid cleavage during isothermal amplification reactions, can also be employed to enhance reaction specificity through their inherent nucleic acid affinity.

Proposed modifications to the EXPAR template involve innovative alterations that aim to effectively inhibit non-specific amplification through modulation of template Gibbs free energy. Additionally, the strategic design of template nucleic acid sequences is envisioned to enhance EXPAR amplification efficiency to some extent. However, meticulous design



and computational analysis are crucial for template development, demanding both high universality for target detection and cost-effectiveness for widespread amplification applications. In contrast, chemical modification of the template primarily targets the mitigation of non-specific interactions arising from the template itself. This method offers advantages in operational simplicity and relatively lower costs. However, its efficacy may not be sufficiently stable, necessitating further mechanistic investigations to improve its robustness.

## EXPAR-based assays incorporating CRISPR/Cas

The Clustered Regularly Interspaced Short Palindromic Repeats (CRISPR)-Cas (CRISPR-associated) system originates from the adaptive immune system of prokaryotes, where it serves as a defense mechanism against invading nucleic acid elements. In recent years, the CRISPR-Cas system has emerged as a powerful tool for gene editing and nucleic acid detection due to its inherent sensitivity, specificity, flexibility, and operational simplicity.<sup>42–44</sup> Notably, the reverse cleavage activities of recently discovered Cas enzymes, such as Cas12a, Cas13a, and Cas14a, have positioned the CRISPR-Cas system as a promising candidate for the development of next-generation

diagnostic biosensing platforms.<sup>45–48</sup> Previous research has demonstrated that combining the CRISPR-Cas system with isothermal amplification techniques offers unparalleled advantages, including exceptional sensitivity, specificity, and portability.<sup>49</sup>

### Cas9

The CRISPR/Cas9 system's ability to perform targeted cleavage in the presence of a specific recognition sequence (PAM) offers a promising approach for reducing non-specific amplification in EXPAR. Capitalizing on this feature, Huang *et al.* proposed a novel nucleic acid detection system (CAS9EXPAR)<sup>50</sup> (Fig. 2A). This system utilizes a pre-assembled Cas9/sgRNA complex, formed by the union of sgRNA and Cas9, to facilitate precise cleavage of the designated target sequence. Unlike conventional nucleic acid amplification methods, CAS9EXPAR enables target-agnostic amplification, eliminating the need for external primers. Furthermore, this technique boasts a detection threshold of 0.82 amol and a runtime of approximately 60 minutes. Notably, it exhibits significantly enhanced specificity and amplification efficacy in discriminating single-base mismatches within target sequences. Building upon this innovation, Wang *et al.* proposed a novel strategy that integrates CAS9EXPAR with G-quadruplex/hemin for visual analysis (Cas-G4EX)<sup>51</sup> (Fig. 2B). This approach achieves a LOD as low as 100 aM for single-stranded DNA (ssDNA) detection. Beyond its

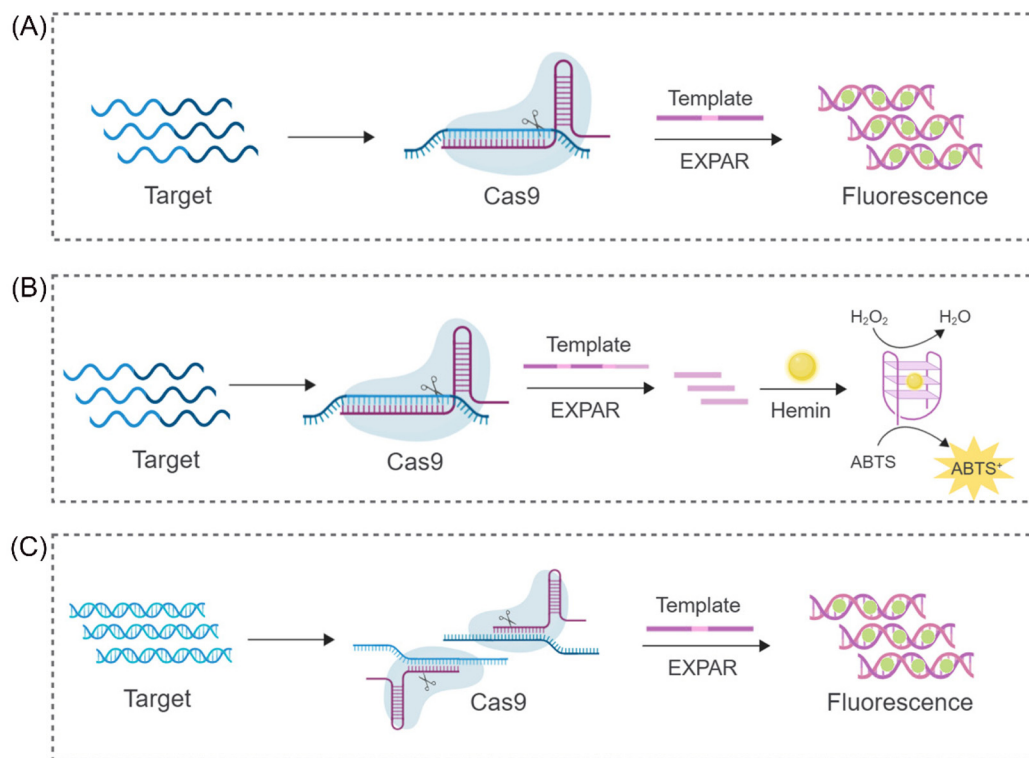


**Fig. 2** Schematic representation of different CRISPR/Cas9-based approaches. (A) A CRISPR/Cas9 triggered exponential amplification method (CAS9EXPAR).<sup>50</sup> (B) A PAMmer-assisted CRISPR/Cas9 system mediated G4-EXPAR (Cas-G4EX) strategy for site-specific detection of ssRNA and ssDNA.<sup>51</sup> (C) A novel method for detecting DNA mutations utilizing EXPAR triggered by double CRISPR-Cas9.<sup>52</sup>





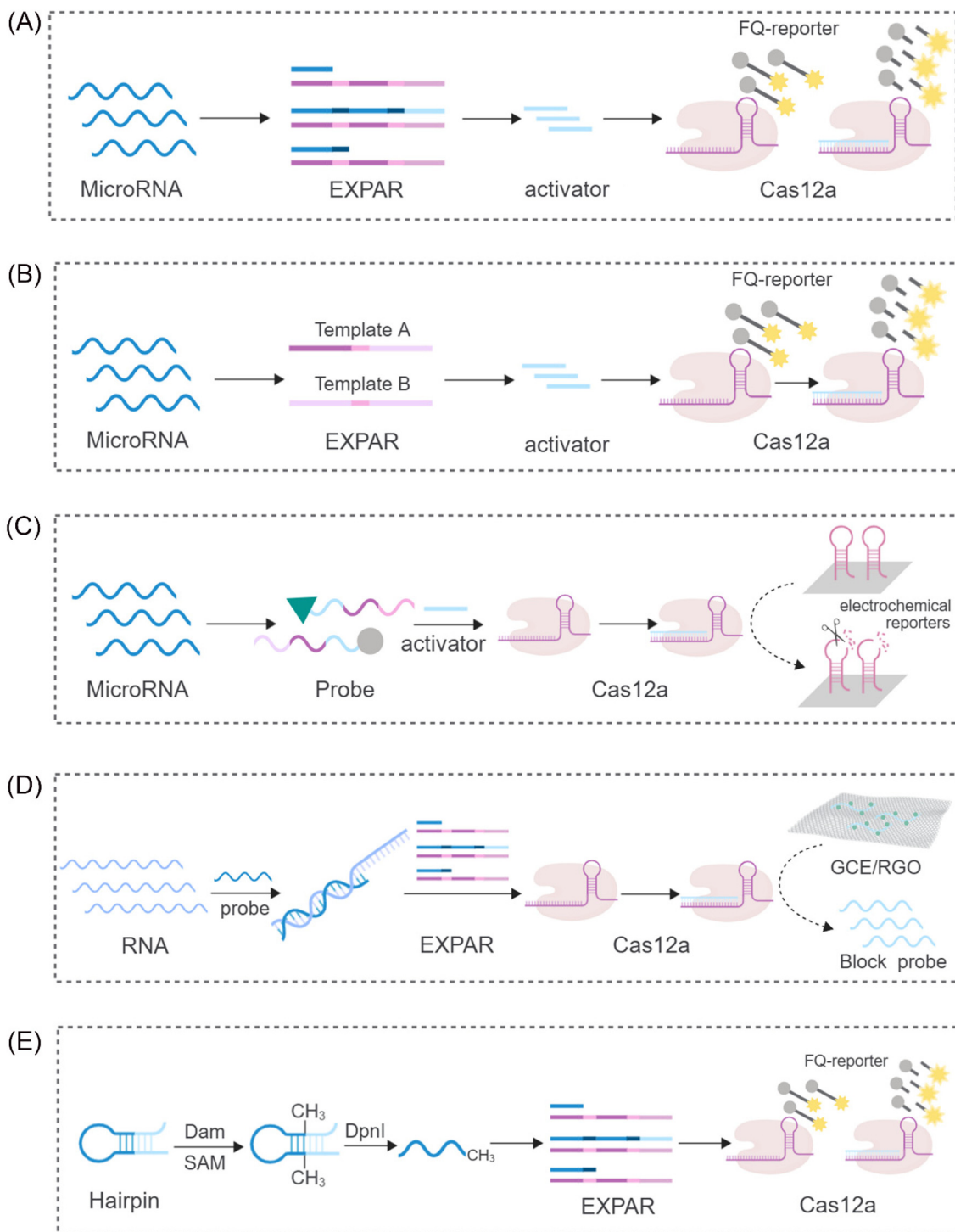


**Fig. 3** Schematic representation of different CRISPR/Cas12a-based approaches. (A) A sensing platform based on CRISPR/Cas12a and EXPAR to realize ultrasensitive analysis of miRNAs.<sup>49</sup> (B) A novel strategy to eliminate the non-specific signal by integrating the CRISPR-Cas12a system into two-template EXPAR.<sup>28</sup> (C) A highly sensitive electrochemical miRNA detection platform based on click chemistry actuated EXPAR and Cas12a.<sup>21</sup> (D) An improved electrochemical sensor based on EXPAR and CRISPR/Cas12a is constructed for sensitive detection of the p53 gene.<sup>58</sup> (E) A fluorescent biosensor based on the EXPAR-initiated CRISPR/Cas12a (EIC) strategy for ultrasensitive DNA methyltransferase detection.<sup>59</sup>

application to oligonucleotide chains, researchers are exploring the use of the CRISPR-EXPAR system for dsDNA detection, particularly in the context of gene mutations. Song's team has proposed a CRISPR-EXPAR gene mutation detection system

that employs a dual Cas9/sgRNA complex<sup>52</sup> (Fig. 2C). This system utilizes two Cas9/sgRNA complexes to cleave specific regions harboring mutations within the target DNA. The method achieved a LOD as low as 437 aM for detecting model



target mutations in the human epidermal growth factor receptor 2 (*EGFR2*) gene. Notably, this approach offers exceptional specificity, circumventing the limitations inherent in conventional gel electrophoresis for confirming the presence of genetic mutations. Similarly, Qin *et al.* recently proposed a strategy based on CRISPR/Cas9-induced isothermal exponential amplification reaction (IEXPAR) for the specific differentiation and detection of antibiotic-resistant bacteria.<sup>53</sup> This approach involves the initial digestion of the target gene segment into two short fragments with free 3' hydroxyl (3'-OH) ends by Cas9. Subsequently, an IEXPAR template (X'-Y-X') designed to target one of the cleaved DNA fragments triggers efficient exponential amplification of the IEXPAR reaction.

### Cas12

While the CRISPR/Cas9 system exhibits high specificity for dsDNA cleavage guided by PAM sequences, the CRISPR/Cas12 system displays a unique characteristic. Upon activation by complementary crRNA-guided ssDNA, it exhibits indiscriminate ssDNA degradation activity. Interestingly, this activity, referred to as *trans*-cleavage activity (side-chain cleavage), is a common feature among all Cas12a homologs, degrading any available ssDNA molecule into mono/dinucleotides.<sup>54,55</sup> This unique property of Cas12a has attracted significant research interest, particularly in its combined application with EXPAR. Yang *et al.* proposed a sensor platform for highly sensitive miRNA analysis that leverages the *trans*-cleavage activity of CRISPR/Cas12a in conjunction with EXPAR<sup>49</sup> (Fig. 3A). Using miR-27a as a model target, they designed an EXPAR template with an AXAXB composition. The presence of miR-27a triggers a cascading EXPAR process, generating many activation fragments. These fragments can then hybridize with the specific crRNA of the CRISPR/Cas12a system, inducing multiple *trans*-cleavage events by Cas12a. Following a similar principle, Huang's team employed Carter *et al.*'s non-reverse transcription EXPAR (RTF-EXPAR) technique<sup>56</sup> to achieve highly sensitive SARS-CoV-2 RNA detection.<sup>57</sup> This method offers several advantages, including rapidity, sensitivity, accuracy, and minimal equipment requirements. Additionally, it can be readily adapted for detecting other RNA targets by simply modifying the RTF converter sequence. However, both aforementioned approaches necessitate the integration of two separate template strands into a single template. This limits the independent adjustment of concentrations for the two functional regions. Furthermore, it can lead to the formation of a significant number of unpredicted secondary structures and a low signal-to-noise ratio (approximately 4) due to non-specific double strands. To address these limitations and eliminate interference caused by non-specific amplification, Niu's research team proposed a novel strategy that integrates the CRISPR-Cas12a system into a dual-template EXPAR system termed EXPCas<sup>28</sup> (Fig. 3B). In this strategy, the Cas12a system functions as a filter, effectively removing non-specific amplification within EXPAR and mitigating its impact. Compared to the previous single-template approach, this method signifi-

cantly improves the signal-to-background ratio, increasing it from 1.3 to 15.4.

Furthermore, Wei *et al.* proposed a novel strategy integrating click chemistry and electrochemistry with CRISPR-Cas systems and EXPAR<sup>21</sup> (Fig. 3C). This approach involves the immobilization of Cas12a with reverse cleavage activity on the surface of an electrode. DNA fragments generated through EXPAR amplification can then activate this immobilized Cas12a, disrupting hairpin DNA on the electrochemical receptor. This disruption results in a subsequent alteration of the electrochemical signal. In the signal detection stage, Zhou *et al.* combined the use of segment probes and electrochemical reactions to achieve sensitive detection of the *p53* gene<sup>58</sup> (Fig. 3D). To enhance the electrochemical signal, these segment probes were captured by a reduced graphene oxide-modified electrode (GCE/RGO). This electrochemical sensor exhibited a limit of detection (LOD) of 0.39 fM, demonstrating a tenfold improvement in sensitivity compared to fluorescence detection methods. These findings suggest that the combination of electrochemical reactions with CRISPR-Cas systems and EXPAR has the potential to significantly improve the sensitivity and amplification efficiency of detection assays.

Beyond its application in nucleic acid detection, the combination of EXPAR and CRISPR-Cas systems has demonstrated significant potential for the detection of diverse molecular biomarkers. Sun *et al.* reported a novel system for sensitive detection of DNA transferase activity that leverages EXPAR initiation by a CRISPR/Cas12a system<sup>59</sup> (Fig. 3E). This system employs a hairpin probe that undergoes methylation by DNA adenine methyltransferase (Dam MTase). Subsequently, DpnI digestion of the methylated probe generates oligonucleotide fragments that can function as primers for EXPAR. Following a similar principle for DNA methylation detection, Wu *et al.* developed a versatile platform for the ultrasensitive detection of CLDN11 methylation.<sup>60</sup> This platform integrates methylation-dependent restriction endonuclease GlnI cleavage with EXPAR and CRISPR-Cas12a, forming the GlnI-EXPAR-Cas12a platform. GlnI recognizes and cleaves methylated target sites, releasing fragments that serve as triggers for the EXPAR-CRISPR/Cas12a system. This platform exhibits a low LOD of  $1.25 \times 10^{-15}$  M and can reliably identify CLDN11 methylation at an abundance of 0.1%, even in the presence of a significant amount of unmethylated fragments.

### Cas13

The CRISPR-Cas13 system comprises a crRNA molecule and an adjacent stem-loop structure known as a direct repeat. Cas13 protein binds to the DR and utilizes it to guide the crRNA towards complementary sequences within the target RNA sample. Upon successful pairing between the spacer sequence within the crRNA and the target RNA, Cas13 cleaves the target RNA at its distal end.<sup>61</sup> This system offers the advantage of targeted ssRNA cleavage without relying on PAM sequences for recognition. Additionally, the CRISPR-Cas13 system exhibits a unique *trans*-activation collateral cleavage activity specific to the target, making it a valuable tool for various applications, including its use as a molecular switch.<sup>62</sup> Capitalizing on



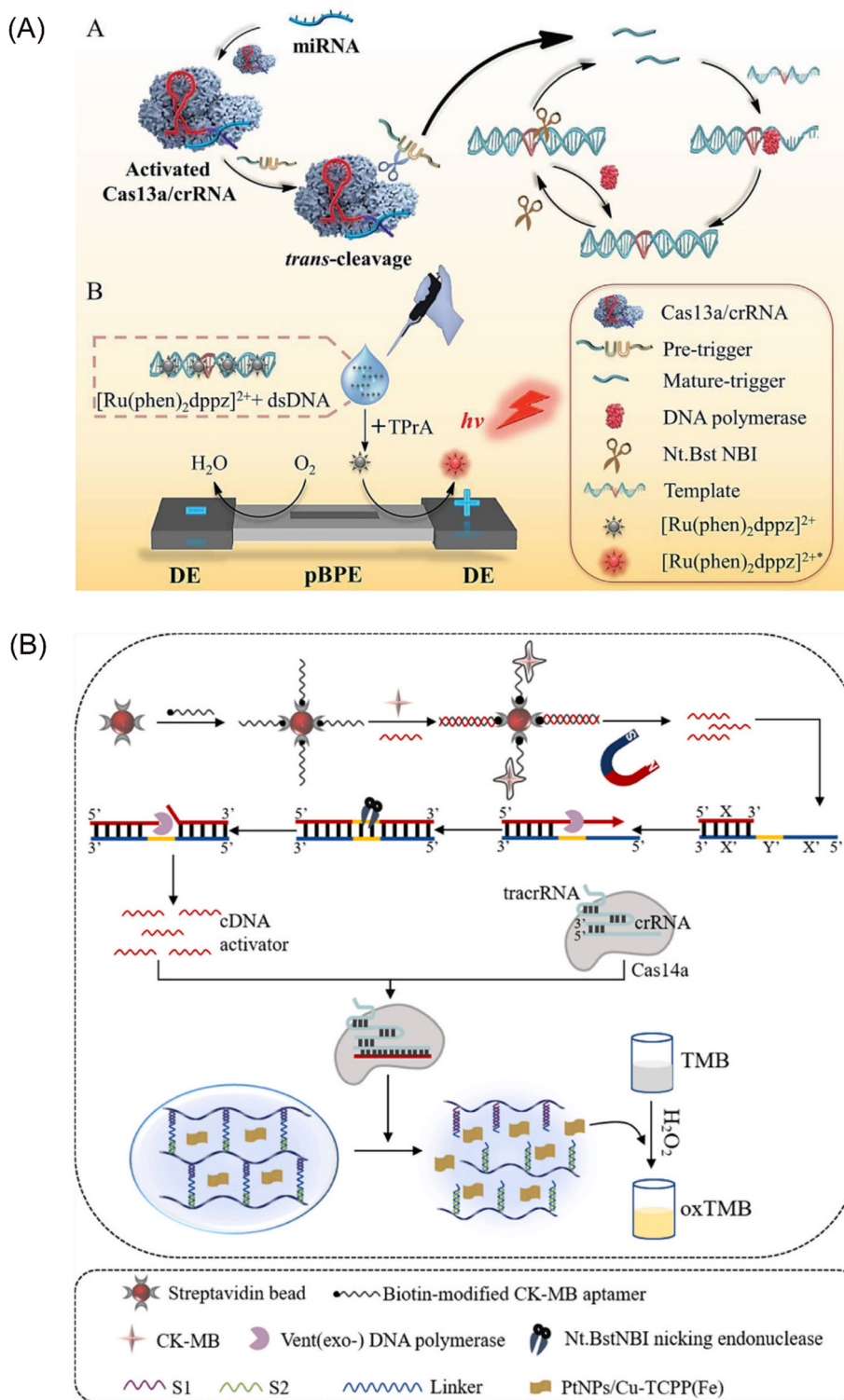


**Fig. 4** Schematic representation of other CRISPR/Cas-based approaches. (A) A CRISPR/Cas13a and EXPAR powered portable electrochemiluminescence chip for ultrasensitive and specific miRNA detection.<sup>45</sup> (B) A programmable non-nucleic acid target detection platform that utilized Cas14a and EXPAR to drive changes in the mechanical properties of a DNA hydrogel.<sup>65</sup>

these features, Zhou *et al.* developed a portable electrochemiluminescence (ECL) chip termed PECL-CRISPR that utilizes CRISPR/Cas13a<sup>45</sup> (Fig. 4A). In this platform, target miRNAs

activate Cas13a, prompting it to cleave a precursor probe. This cleavage event triggers subsequent exponential amplification and detection *via* ECL. Notably, incorporating the photosensi-



tive molecule,  $[\text{Ru}(\text{phen})_2\text{dppz}]^{2+}$ , eliminates the need for cumbersome electrode modifications and washing steps, further streamlining the assay. These advancements highlight the significant potential of CRISPR-Cas13 as a powerful tool for EXPAR-based molecular diagnostics.

### Cas14

CRISPR-Cas14a represents the smallest RNA-guided nuclease discovered to date. This compact system offers targeted cleavage of specific sites without requiring a PAM (protospacer adjacent motif) structure, making it distinct from other CRISPR-Cas systems.<sup>63</sup> Furthermore, it exhibits high fidelity and enhanced specificity in recognizing single-stranded DNA (ssDNA) substrates.<sup>64</sup> Chen *et al.* proposed a novel strategy that leverages the anti-sense cleavage activity of CRISPR-Cas14a to activate DNA hydrogels for ultrasensitive detection of creatine kinase-MB (CK-MB), a biomarker indicative of myocardial infarction<sup>65</sup> (Fig. 4B). The activation of the CRISPR-Cas14a system is achieved by introducing competitive dissociation and complementary DNA (cDNA) from the EXPAR. Subsequently, the activated Cas14a protein non-specifically cleaves the crosslinker chains within the DNA hydrogel. This cleavage event triggers the release of pre-embedded PtNPs/Cu-TCPP(Fe) nanoparticles, leading to a series of observable changes in absorbance. These absorbance changes can then be quantitatively analyzed to enable sensitive detection of CK-MB. This innovative approach represents the first integration of CRISPR-Cas14a with DNA hydrogels. It offers the advantages of enhanced programmability for DNA hydrogels and facilitates the visualization of detection results.

Integrating CRISPR-Cas systems into EXPAR offers several advantages that hold promise for clinical applications. Firstly, it introduces a novel recognition mechanism based on specific nucleic acid sequence binding. This significantly improves the specificity of EXPAR compared to that of traditional methods. Secondly, the anti-sense cleavage activity of Cas proteins provides a unique signal amplification method within the EXPAR. This plays a crucial role in enhancing the overall sensitivity of the assay. Lastly, Cas proteins exhibit enzymatic activity towards DNA or RNA strands at physiological temperatures (37 °C). Their excellent compatibility with IAT allows for seamless integration into EXPAR. However, a key challenge associated with this approach is the potential for non-specific cleavage by Cas proteins on non-target nucleic acid segments. Many current methods address this issue by employing a two-step strategy. Although effective, this approach can lead to increased reaction complexity and reduced user-friendliness. Therefore, future advancements should focus on simplifying the amplification strategy of CRISPR-Cas systems within EXPAR to facilitate its broader adoption in clinical settings.

## EXPAR-based assays incorporating aptamers

Aptamers are short nucleic acid strands with specific recognition functions selected through exponential enrichment

systems. The main functions are as novel recognition ligands with high specificity and affinity towards their targets. They possess characteristics such as easy synthesis, programmability, site-specific labeling, and long-term storage, making them compatible with various signal patterns and allowing for signal amplification. These features demonstrate their unique advantages in biosensing and molecular diagnostics.<sup>66–68</sup> With the continuous emergence of new aptamers, the detectable target range of aptamer sensors based on EXPAR is expanding. In these EXPAR-based aptamer sensors, the aptamer usually serves as the recognition molecule, while EXPAR acts as the signal amplification tool, combining the high specificity of the aptamer with the high amplification efficiency of EXPAR for the detection of small molecule biomarkers.

Yu *et al.* developed a novel electrochemical biosensing platform for protein analysis that utilizes target-triggered proximity hybridization-mediated EXPAR<sup>69</sup> (Fig. 5A). This platform integrates a protein recognition adapter into the DNA probe. Upon recognition of the target protein by the adapter, it triggers DNA strand displacement by increasing the local concentration of the probe. The displaced DNA molecules can then hybridize with double-stranded probes immobilized on the electrode surface. This hybridization event initiates EXPAR and subsequently leads to the cleavage of the double-stranded probes. Liao *et al.* proposed a modular signal amplification system that combines an aptamer, a hammerhead ribozyme, EXPAR, and horseradish peroxidase (HRP) activity with the substrate 3,3',5,5'-tetramethylbenzidine (TMB)<sup>70,71</sup> (Fig. 5B). Ligand-aptamer binding triggers conformational changes and self-cleavage of the ribozyme. This cleavage event then initiates the exponential amplification of the reporter sequence during the EXPAR process. This three-level detection system constitutes a versatile platform. It can be readily modified for the detection of virtually any chosen analyte target within a time-frame of 5 to 10 minutes.

Zhang *et al.* proposed an aptamer-based analytical approach for detecting the mycotoxin T-2. This approach integrates EXPAR with fluorescent silver nanoclusters (AgNCs) for sensitive detection.<sup>72</sup> The method utilizes aptamer-conjugated magnetic beads (MNBs) functionalized with cDNA. Free T-2 in the sample competes with the immobilized cDNA for binding to the aptamers. Following magnetic separation, the isolated DNA fragments serve as primers to initiate EXPAR amplification of ssDNA. The resulting ssDNA can then interact with  $\text{Ag}^+$  ions to form fluorescent AgNCs. This fluorescence generation enables highly sensitive detection of T-2, with a LOD as low as  $30 \text{ fg mL}^{-1}$ . Due to its high sensitivity, this approach holds promise for rapid detection applications in the context of infectious diseases caused by microorganisms.

Xu *et al.* further established a visually detectable analytical sensing method for *Brucella suis* detection based on a biohybrid interface.<sup>73</sup> This method leverages aptamer incorporation to achieve target-specific recognition. Upon successful target binding, an antibody-target-fusion aptamer immunosandwich structure is formed. Subsequent EXPAR activation leads to the assembly of a G-quadruplex structure. This structure can





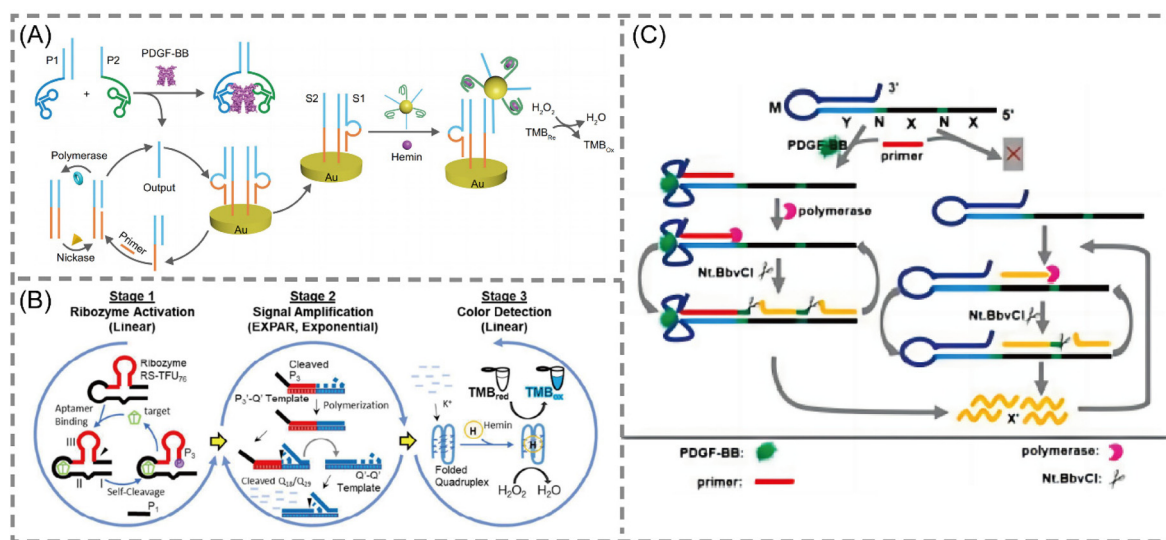


**Fig. 5** Schematic representation of aptamer-based approaches. (A) A novel electrochemical biosensing platform on the basis of target-triggered proximity hybridization-mediated EXPAR for ultrasensitive protein analysis.<sup>69</sup> (B) A simple colorimetric system for detecting target antigens by a 3-stage signal transformation-amplification strategy.<sup>70,71</sup> (C) A rationally designed aptamer-based hairpin structure-switching EXPAR template for realizing protein triggering EXPAR (PTEXPAR).<sup>74</sup>

then be detected colorimetrically through a reaction with G4/hemin deoxyribonuclease. Under optimized conditions, the assay enables visual analysis within 2 hours and achieves a LOD of 2 cfu mL<sup>-1</sup> for pure cultures. Notably, this method eliminates the need for DNA extraction, cultivation, and expensive instrumentation. Consequently, it presents a promising strategy for real-time point-of-care microbial detection.

Intriguingly, Chen *et al.* developed a protein-triggered (PT)-EXPAR method using a rationally designed aptamer-based hairpin structure conversion template<sup>74</sup> (Fig. 5C). This approach initially features a stem-loop hairpin structure formed by the recognition region of the aptamer. This configuration prevents hybridization between the triggering region and the EXPAR primer. In the presence of the target protein, the aptamer undergoes conformational changes to specifically recognize and bind to the target. This binding event exposes the triggering region, allowing the primer to bind and initiate EXPAR. This PT-EXPAR method facilitates label-free and wash-free one-pot quantitative detection of PDGF-BB with high sensitivity. The assay achieves a detection limit as low as 4.9 fM within 30 minutes and boasts a dynamic range spanning seven orders of magnitude. Due to the inherent high affinity and specificity of aptamers, the method exhibits remarkable selectivity and can effectively distinguish between dimeric isoforms of PDGF proteins. Furthermore, by adapting the corresponding aptamer recognition sequences, PT-EXPAR can be established as a universal platform for detecting diverse protein targets. This approach is promising for generating valuable information in biomedical research and clinical diagnostics.

The sensing principle of aptamer-based EXPAR systems primarily relies on the structural conversion of the aptamer to

trigger EXPAR amplification. This approach leverages the specific recognition mechanism of aptamers to address the potential issue of non-target triggering in EXPAR. Furthermore, the high affinity of aptamers enables stable binding to various targets, including proteins. This binding event facilitates the conversion of protein signals into nucleic acid signals, ultimately achieving the versatility of EXPAR detection for diverse analytes. However, challenges remain regarding the clinical translation of aptamer-based EXPAR. One such challenge is the limited availability of aptamers with optimal performance. While numerous aptamers targeting various disease markers have been reported and are accessible through resources like the Aptagen database (<https://www.aptagen.com/>), a comprehensive characterization of most aptamers is lacking. Consequently, only a few reported aptamers have received approval for use in biotechnology or clinical settings. To enable comprehensive detection of small molecule biomarkers, the development of a broader library of well-characterized aptamers is necessary.

## EXPAR-based assays incorporating IATs

To further augment the signal amplification capabilities of EXPAR, a growing number of researchers are exploring the integration of EXPAR with other isothermal amplification techniques. This approach results in a cascade amplification effect, where EXPAR primarily functions in the upstream signal pathway to exponentially enrich the signal. The enriched ssDNA fragments then trigger subsequent downstream isothermal amplification processes. Among IATs,



hybridization chain reaction (HCR), strand displacement amplification (SDA), and catalytic hairpin assembly (CHA) are widely employed in cascade amplification reactions with EXPAR due to their simple reaction components and high amplification efficiency.<sup>75–80</sup> This seamless and effective combination with EXPAR has been extensively applied to significantly enhance the sensitivity and specificity of detection assays.

### HCR

HCR offers a unique approach for achieving ultra-high detection sensitivity comparable to PCR. This unlabeled nucleic acid amplification method is both simple and cost-effective, eliminating the need for enzymes. HCR significantly simplifies detection systems, making it an ideal signal amplification platform. A key advantage of HCR over other isothermal amplification techniques is its enzyme-free nature. This characteristic translates to exceptional tolerance to environmental interference, enabling target detection in complex real-world samples, even within live cells or organisms.<sup>81</sup> HCR is the foundation for numerous detection strategies targeting DNA, RNA, proteins, and small molecules. However, HCR-based amplification faces inherent challenges. Currently, most HCRs operate in a one-dimensional manner. The linear amplification achieved by HCR alone is insufficient for detecting very low target concentrations. Consequently, additional nucleic acid amplification procedures are often necessary to enhance detection sensitivity in bioassays.<sup>82,83</sup> EXPAR offers a solution to this limitation. The abundant ssDNA generated during the exponential first step of EXPAR can function as an activating sequence to trigger HCR amplification. In the presence of a high quantity of ssDNA, HCR undergoes rapid amplification, effectively overcoming the limitation of linear growth inherent to HCR alone. Therefore, the combination of EXPAR's exceptional exponential signal amplification capability with the efficient, enzyme-free characteristics of HCR leads to a significant improvement in overall amplification efficiency and detection sensitivity.

Xu *et al.* developed an electrochemical biosensor for copper (II) ion detection that leverages Cu<sup>2+</sup>-dependent DNAzyme (cDNAzyme), EXPAR, and HCR.<sup>84</sup> EXPAR functions as a bridge between the cDNAzyme recognition platform and the HCR amplification platform. It facilitates the enrichment of single-stranded oligonucleotides onto a designated DNA sequence. This platform achieves high signal specificity and sensitivity through a two-step signal amplification process coupled with an intelligent nanofluidic gating system. In another approach, Wang *et al.* constructed a novel cascade amplification strategy utilizing fluorescence as the output signal<sup>85</sup> (Fig. 6A). This method employs magnetic beads functionalized with E2 and complementary DNA as a competitor. The presence of free complementary strands in the supernatant serves as the triggering sequence to initiate EXPAR, leading to the generation of a significant quantity of ssDNA sequences. These ssDNA sequences then facilitate HCRs, unfolding hairpin structures, and subsequent fluorescence recovery. This practical approach

holds promise for diverse applications, including protein and nucleic acid screening, as well as quantitative analysis.

Building upon the exceptional performance of EXPAR-HCR cascade amplification, researchers have explored its application in DNA mutation detection. Tang *et al.* recently introduced a highly sensitive method for *BRCA1* gene detection that leverages a dual amplification strategy combining EXPAR and HCR.<sup>83</sup> This approach integrates HCR probes and introduces a trigger probe to initiate EXPAR on a 96-well microtiter plate. Amplified signal quantification is achieved using a spectrophotometer, where horseradish peroxidase (HRP) catalyzes the reaction with a TMB substrate. This dual amplification approach demonstrates a favorable linear range spanning from 0.1 fM to 100 pM, achieving a LOD as low as 74.48 aM. The versatility of this novel DNA detection method suggests its potential as a high-throughput platform for detecting various targets, including cancer biomarkers, genetic diseases, drug resistance mutations, and infectious agents.

### CHA

CHA represents an enzyme-free DNA circuit that amplifies signals through a thermodynamically driven process favoring increased entropy. Notably, CHA relies solely on the design of intermolecular base pairing. Requiring only ssDNA or RNA as input, CHA utilizes cyclic utilization to catalyze the opening of two metastable DNA hairpins. This process enables exponential amplification of the target sequence within a short time-frame, typically 15 minutes.<sup>86,87</sup> Several key attributes contribute to the widespread adoption of CHA: its rapid, enzyme-free nature, straightforward design principles, high degree of adaptability, minimal background noise, and efficient signal conversion.<sup>88,89</sup> These characteristics allow for the seamless integration of CHA with other isothermal amplification reactions, which often operate under different temperatures, buffers, and enzyme requirements.<sup>80</sup> Therefore, combining CHA and EXPAR in a cascade amplification system eliminates the need for enzyme introduction while maintaining exceptional amplification performance. This makes CHA an ideal choice for enhancing the sensitivity and specificity of the EXPAR.

Tang *et al.* developed a rapid point-of-care lateral flow biosensor for universal protein detection by integrating EXPAR and CHA technologies. This innovative platform leverages a proximity hybridization-mediated protein–DNA transducer to convert the protein signal into a DNA signal<sup>90</sup> (Fig. 6B). This conversion triggers the opening of an ssDNA capture probe, initiating the EXPAR process. The enriched ssDNA product is subsequently amplified through CHA, generating dsDNA products. Utilizing the lateral flow biosensor format, these dsDNA products can be detected within a timeframe of 5 minutes. The assay boasts a dynamic detection range spanning from 1 fM to 100 nM, with a LOD as low as 0.74 fM. Notably, the incorporation of EXPAR technology has led to a near-tenfold improvement in sensitivity compared to those of previously reported methods. This demonstrates the high sensitivity and efficiency of the combined EXPAR-CHA approach, offering a



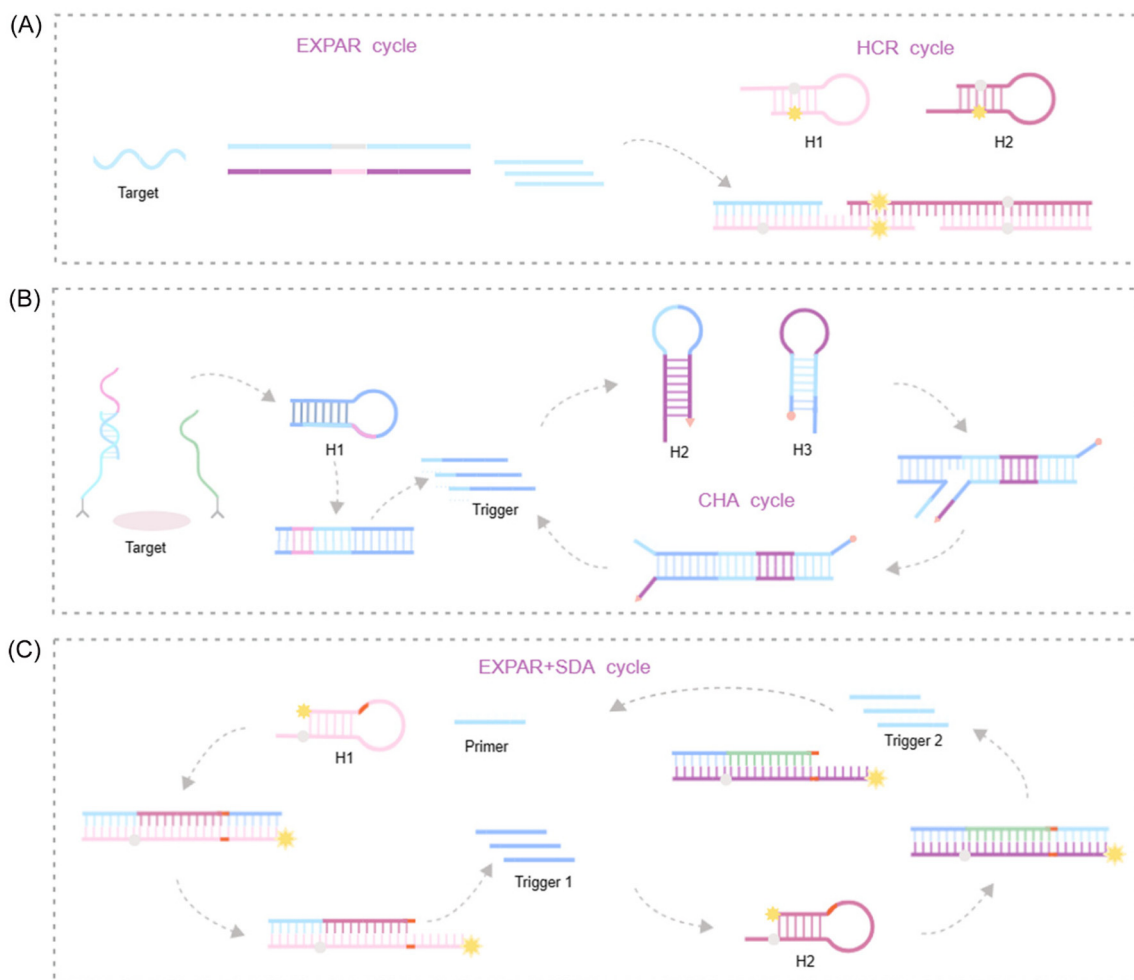


**Fig. 6** Schematic representation of IAT-based approaches. (A) HCR-based: a fluorescence amplification strategy for high-sensitivity detection of 17 beta-estradiol based on EXPAR and HCR.<sup>85</sup> (B) CHA-based: a lateral flow biosensor for universal protein detection based on a proximity hybridization mediated protein-to-DNA signal transducer and isothermal exponential amplification.<sup>90</sup> (C) SDA-based: primer dephosphorylation-initiated circular exponential amplification for ultrasensitive detection of alkaline phosphatase.<sup>94</sup>

promising strategy for universal and straightforward protein detection.

### SDA

SDA represents an entropy-driven nucleic acid amplification technique offering several advantages, including operational simplicity, isothermal reaction conditions, rapid amplification kinetics, and high sensitivity. Significantly, SDA also demonstrates compatibility with diverse signal probes. In a typical SDA reaction, target-mediated hybridization triggers the extension of primer sequences along a predetermined template. Notably, the target can be displaced by another generated DNA fragment before subsequent hybridization events, leading to further rounds of SDA amplification. This unique characteristic positions SDA as a promising signal amplification technique, finding widespread application in sensitive detection of nucleic acids, proteins, and small molecules.<sup>91</sup> Furthermore, SDA can be readily integrated with various biosensor formats,

including colorimetric, fluorescence, and chemiluminescence methods. The combination of SDA with other amplification strategies, particularly in a cascade format, has garnered significant interest due to its potential benefits. In this approach, the products generated from the upstream reaction serve as triggers to initiate the downstream reaction. Compared to traditional exponential amplification techniques, cascade amplification offers the advantage of not only achieving higher signal intensity but also maintaining lower background noise.<sup>78,79,92</sup> By integrating SDA with EXPAR, this approach facilitates a significant enhancement in both detection specificity and sensitivity.

The SDA-EXPAR strategy leverages the ssDNA output from the upstream SDA unit as the target to activate the downstream EXPAR unit. This continuous and repetitive hybridization process results in secondary signal amplification. In a study by Wang *et al.*, a highly sensitive fluorescence method was developed for detecting alkaline phosphatase (ALP) activity based



on primer-initiated isothermal exponential amplification.<sup>93</sup> The researchers designed two bifunctional hairpin probes that served as both templates for EXPAR and generators of signal output. Following the initiation of two consecutive SDAs, the accumulated signal further triggered a circular EXPAR, resulting in a cascade amplification of fluorescence signals. This study demonstrated exceptional sensitivity, achieving a LOD of  $2.0 \times 10^{-10}$  U  $\mu\text{L}^{-1}$  and a dynamic range spanning five orders of magnitude ( $1.0 \times 10^{-9}$  to  $1.0 \times 10^{-4}$  U  $\mu\text{L}^{-1}$ ). This sensitivity allows for ALP detection at the single-cell level. Importantly, this method holds promise for measuring kinetic parameters and screening potential inhibitors, making it a powerful approach for ALP-related biomedical research and clinical diagnostics. Building upon this approach, researchers further introduced T7 exonuclease-assisted cyclic signal amplification into the system, developing a sensitive fluorescence method for detecting DNA glycosylase activity<sup>94</sup> (Fig. 6C). This method utilizes target-induced ligation-dependent three-circle cascade amplification. DNA glycosylase activity triggers the cleavage of damaged bases within the hairpin substrates, sequentially activating ligation-dependent SDA and EXPAR. Subsequently, T7 exonuclease-assisted cyclic signal amplification enhances the fluorescence signal. This three-circle cascade amplification strategy exhibits high efficiency and low background signals due to the effective inhibition of non-specific amplification. Notably, this method can be performed in a homogeneous solution, eliminating the need for complex separation steps. This approach offers a novel strategy for DNA glycosylase-related biomedical research.

Integrating different IATs presents a promising approach to overcoming limitations inherent to single IATs in facilitating communication between catalysts and driving cascade biotransformation events. A critical requirement for achieving cascade amplification in isothermal systems is that the product generated by the upstream method serves as a trigger for the downstream method, functioning as a bridge to connect these individual modules. Beyond signal amplification, cascade amplification offers a valuable approach for information transmission and signal transduction. By strategically combining different IATs, cascade amplification strategies can achieve highly sensitive detection while mitigating challenges associated with individual IATs, such as false positives, limited compatibility with specific nucleic acid sequences, and restricted signal amplification capacity. Despite significant advancements, several key issues warrant further consideration in the context of cascade amplification. First, it is crucial to optimize the number of cascade layers and the corresponding reaction time. As the number of cascade layers increases, the detection time increases exponentially. Therefore, establishing an optimal efficiency curve for cascade amplification is paramount. Second, there remains a need to design more efficient cascade sequences that seamlessly integrate different isothermal amplification methods. Even when employing the same IAT, recognition and reaction processes can differ for nucleic acids with varying lengths and sequence information.

## EXPAR-based assays incorporating metal nanoclusters

Metal nanoclusters represent a class of ultrasmall nanoparticles with diameters ranging from sub-nanometers to 2 nanometers. Notably, they exhibit unique fluorescence properties. Furthermore, MNCs possess many attractive characteristics, including small size, excellent biocompatibility, strong stability, unique catalytic activity, long luminescence lifetime, intense photoluminescence, water solubility, and ease of synthesis. By capitalizing on these advantageous properties, MNCs find applications in diverse fields such as biosensing, therapeutic diagnostics, bioimaging, and biomarker detection.<sup>95–97</sup> Among various MNCs, silver nanoclusters (AgNCs) and gold nanoclusters (AuNCs) are the most widely employed due to their facile synthesis and exceptional antioxidant stability.<sup>98,99</sup> Recognizing the unique photophysical properties of AgNCs and AuNCs, researchers have explored their integration with the EXPAR technique. This integration facilitates the conversion of EXPAR products into detectable signals, enabling more convenient detection schemes, including even visual analysis.

### AuNPs

AuNPs have gained widespread application in colorimetric detection methods for various targets, including DNA, proteins, metal ions, small molecules, and DNA-binding compounds.<sup>100</sup> Jiang *et al.* introduced a colorimetric assay for miRNA detection that leverages the combined power of EXPAR and AuNP-labeled DNA probes<sup>101</sup> (Fig. 7A). This approach transforms the miRNA signal into a reporter molecule (Y) via EXPAR. Subsequently, Y undergoes sandwich hybridization with AuNP-labeled DNA probes, changing the color from red to purple. Notably, this method exhibits high sensitivity, boasting a detection range of 1 aM to 1 nM and a LOD as low as 4.176 aM. These characteristics suggest its potential as an ideal method for diverse applications, including biomedical research, clinical diagnosis, and even field-based diagnostics or monitoring projects. Similarly, Wei *et al.* proposed a novel miRNA detection method that combines EXPAR with AuNPs, employing three-stranded DNA-mediated AuNP assembly.<sup>102</sup> This approach utilizes triple-stranded DNA to induce the aggregation of two types of AuNPs, which can be quantified using UV-Vis spectroscopy. Another study explored a DNA walker based on pre-assembled AuNP probes to trigger the EXPAR.<sup>103</sup> Notably, the freezing techniques employed in the DNA walker construction endow the AuNP probes with exceptional structural stability. Following the “recognition–cleavage–relative motion” cycle of the DNA walker reaction, the system initiates the exponential amplification process.

### AgNCs

DNA-templated silver nanoclusters (DNA-AgNCs) have emerged as a promising material due to their readily tunable fluorescence emission, straightforward synthesis, and excellent





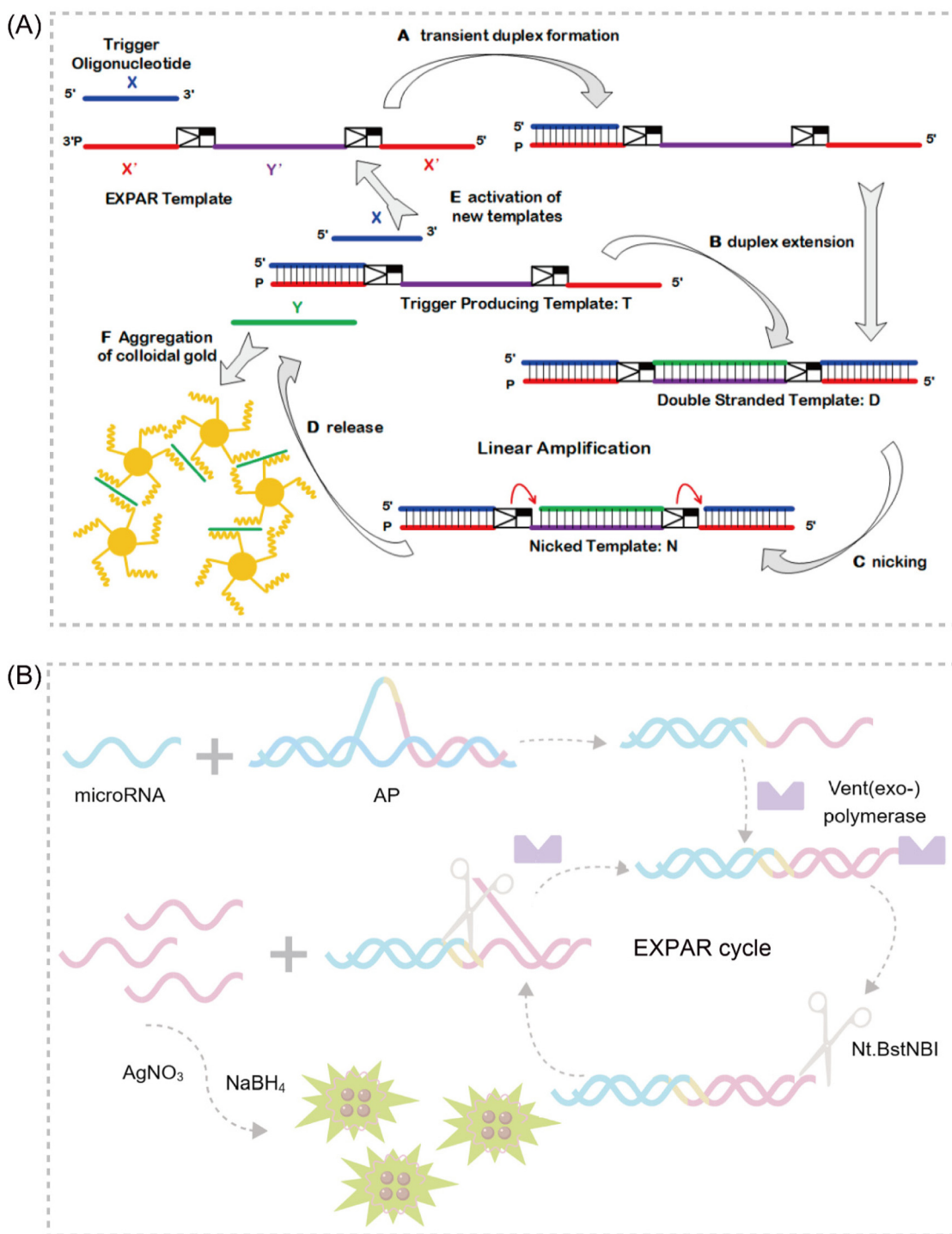


Fig. 7 Schematic representation of MNC-based approaches. (A) A novel design combining EXPAR and gold-nanoparticle visualization for the detection of miRNAs.<sup>101</sup> (B) Fluorometric determination of miRNAs using arch probe-mediated EXPAR combined with DNA-templated silver nanoclusters.<sup>106</sup>

biocompatibility.<sup>104</sup> A particularly attractive feature of DNA-AgNCs is the ability to rationally control their desired photophysical properties by simply modifying the length or sequence of the template DNA. This approach eliminates the need for complex covalent attachment of different fluorescent

materials.<sup>105</sup> Capitalizing on these advantages, Wu *et al.* proposed a highly sensitive fluorescence method for miRNA-141 determination that combines arch probe-mediated EXPAR with DNA template silver nanoclusters<sup>106</sup> (Fig. 7B). This strategy utilizes two arch probes as exponential amplification tem-



plates, enabling the conversion of miRNA-141 into many reporter sequences *via* EXPAR. DNA-AgNCs serve as fluorescence signal carriers, allowing for distinct signal detection.

EXPAR-based sensing platforms that leverage MNCs as signal transducers offer a valuable approach for detecting small molecule biomarkers. This approach eliminates the complex labeling procedures typically associated with traditional fluorescence EXPAR sensing methods. The synergy between EXPAR and metal nanoclusters enhances sensitivity and specificity in small molecule biomarker detection. Additionally, these enzyme-free assays are designed for operational simplicity, making them well-suited for potential clinical diagnostic applications. However, a key challenge impeding broader application lies in the development of an effective and versatile strategy for the preparation of diverse MNCs. This area is expected to be a major focus of future research efforts.

## EXPAR-based assays incorporating enzymes

In the context of EXPARs, enzymes are frequently classified into two categories based on their chemical composition: DNAzymes, which are nucleic acid-based catalysts, and nucleases, which are primarily protein enzymes. Notably, both categories utilize nucleic acids as their substrates. Despite their compositional differences, both DNAzymes and nucleases exhibit remarkable catalytic activity and possess unique biorecognition capabilities. These properties make them particularly well-suited for signal amplification in DNA biosensor applications.<sup>107</sup>

### DNAzymes

Deoxyribozymes, or DNAzymes, represent a unique class of catalytic DNA molecules capable of facilitating various chemical reactions. Their inherent sequence-dependent binding properties allow for facile adaptation to diverse target analytes by modifying the recognition sequences. Mimicking the catalytic activity of proteases, DNAzymes can mediate various chemical reactions, including DNA cleavage and ligation. Several key advantages contribute to the widespread application of DNAzymes as signal amplifiers in isothermal amplification strategies for detecting various targets, including proteins, DNA, and metal ions. These advantages include high catalytic activity, affordability, exceptional thermal stability, minimal non-specific adsorption, and ease of preparation and adaptation.<sup>108–111</sup> In recent years, IATs that integrate the DNAzyme cascade EXPAR as a signal amplification tool have garnered significant attention due to their exceptional sensitivity, operational simplicity, and many other advantages. Broadly, two primary strategies exist for combining DNAzymes and EXPAR to construct biosensors. The first strategy involves initiating EXPAR to generate a DNAzyme (EXPAR-DNAzyme). Conversely, the second strategy utilizes the remaining substrate strand obtained from the DNAzyme cleavage reaction to trigger EXPAR (DNAzyme-EXPAR).

Li *et al.* introduced a novel strategy for sensitive colorimetric detection of target HIV-DNA by incorporating G-triplet (G3) structures into EXPAR amplification products.<sup>112</sup> The cascade EXPAR cycle generates a substantial number of short G-rich sequences, which self-assemble into G3 structures. These G3 structures then bind to heme chloride, forming a G3/heme chloride DNAzyme complex. This approach boasts a detection range spanning from  $1 \times 10^{-13}$  M to  $1 \times 10^{-10}$  M, with a LOD as low as 4.7 fM. Notably, this strategy demonstrates significantly enhanced sensitivity compared to the conventional G-quadruplex/heme-based DNAzyme-integrated EXPAR approach. This work represents a significant advancement in ultrasensitive biosensing and contributes to a deeper understanding of the G3 structure while also opening doors for future G3 applications. Building upon this concept, Yang *et al.* reported an EXPAR strategy that utilizes DNAzyme as the template<sup>113</sup> (Fig. 8A). In this approach, the DNAzyme specifically recognizes  $Pb^{2+}$  within the reaction system, while the G-quadruplex structure serves the function of signal detection.

Gao *et al.* established a label-free electrochemical analysis method for fat mass and obesity-associated protein (FTO) detection, capitalizing on a target-promoted DNAzyme-specific activation strategy coupled with self-triggered exponential amplification reaction (SPEXP) cycling and DNA sandwich assembly.<sup>114</sup> This approach leverages FTO's demethylase activity. FTO catalyzes the removal of methyl groups, thereby restoring the DNAzyme's cleavage activity. This restoration triggers the cleavage of relevant substrates, initiating SPEXP cycling and generating abundant ssDNA. This method presents a novel alternative for detecting multifunctional methyltransferase/demethylase molecules in disease diagnosis and biological research applications<sup>114</sup> (Fig. 8B).

DNAzymes offer several advantages that make them well-suited for bioimaging applications. These advantages include the ease of synthesis and modification, along with exceptional stability across a broad temperature range. Additionally, the DNAzyme cascade EXPAR method facilitates the flexible and ultrasensitive detection of various small molecule markers. Furthermore, DNAzymes exhibit low toxicity and excellent biocompatibility, which are crucial attributes for bioimaging applications. However, the current repertoire of DNAzyme species remains limited. As a result, developing DNAzymes with multifunctional capabilities will likely be a key focus of future research efforts in this field.

### Nucleases

Nucleases are a class of enzymes that play a critical role as analytical tools in DNA biosensor development. These enzymes can be categorized based on their target recognition and cleavage specificities. Restriction enzymes exhibit high sequence specificity, cleaving DNA only at defined recognition sites. In contrast, other nucleases demonstrate less stringent sequence requirements but may recognize specific structural features within their DNA substrates. The presence or absence of a target molecule can influence the generation or disappearance of restriction enzyme recognition sites. This



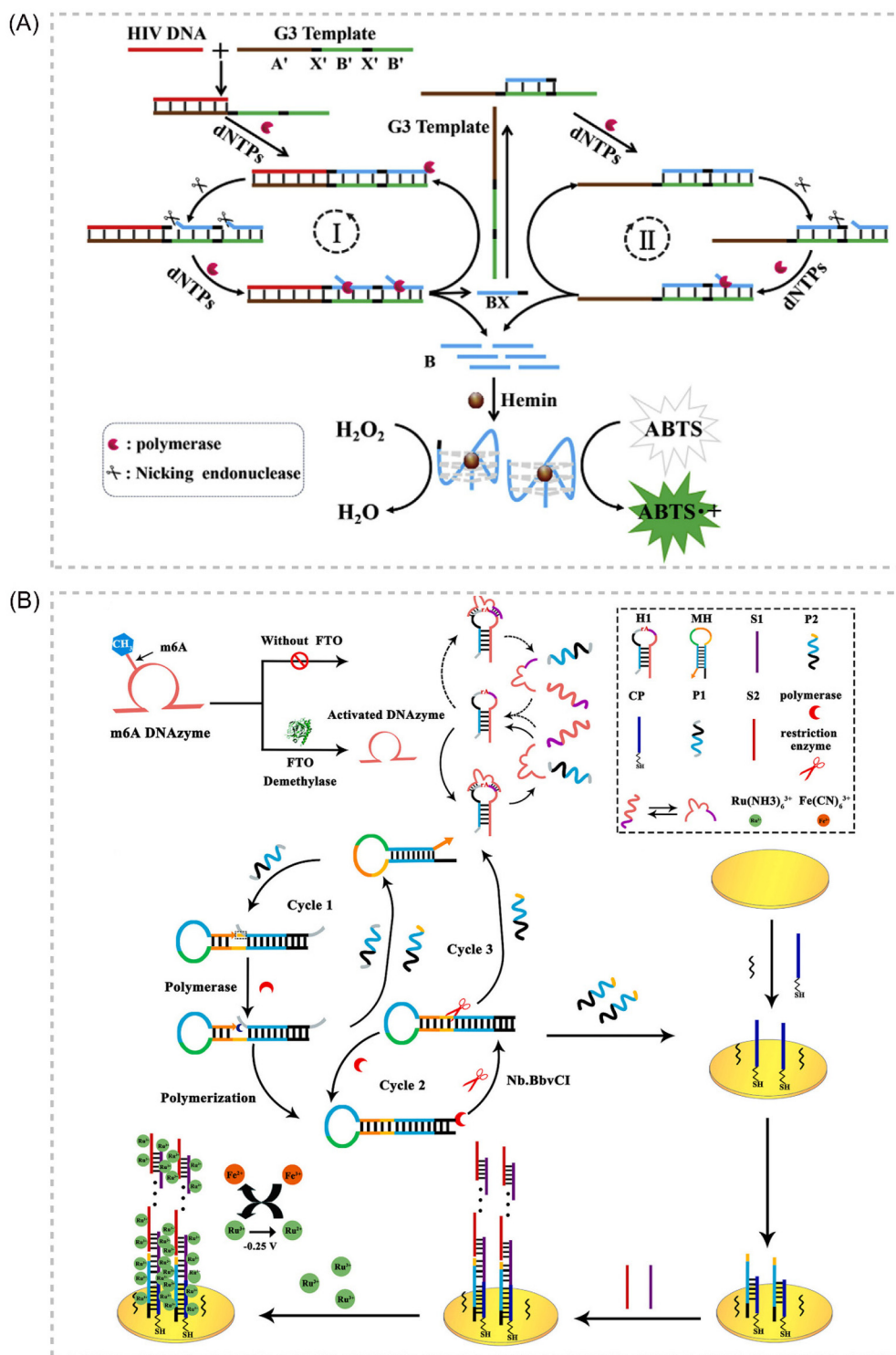


**Fig. 8** Schematic representation of DNAzyme-based approaches. (A) An EXPAR-based biosensing platform for colorimetric detection of target HIV-DNA by incorporating G3 structures in amplification products.<sup>113</sup> (B) Electrochemical FTO assay approach based on a target-promoted specific activation of DNAzyme strategy coupled with self-primer EXPAR cycles and DNA supersandwich assemblies.<sup>114</sup>

phenomenon makes nucleases valuable tools for signal amplification in biosensing applications. Furthermore, nucleases can be further classified based on their cleavage site preferences within the DNA substrate. These categories include

double-strand-specific nucleases, nucleic acid exonucleases, nucleic acid endonucleases, and other nucleases.<sup>107</sup>

**Upstream specific recognition.** A key feature of many EXPAR-based strategies is the utilization of nucleases for



specific upstream recognition events. Capitalizing on the inherent specificity and robustness of nucleases, Professor Zhou's team developed aligner-mediated cleavage-triggered exponential amplification (AMCMD). This innovative method integrates NEases and hairpin probes in a precisely programmable manner, enabling the discrimination of single-base mismatches within target sequences<sup>25,115</sup> (Fig. 9A). AMCMD effectively aligns the enzyme to a specific target site and facilitates precise cleavage at a predetermined position. The short sequence generated by AMCMD then serves as the trigger for the downstream EXPAR, achieving a LOD as low as 1 pM.

Several research groups have made significant advancements in exploiting the EXPAR system for RNA detection. Notably, Yuan's and Chang's teams independently integrated the *Thermoanaerobacter thermophilus* AGO protein (TtAgo) and RNase H into the upstream pathway of EXPAR<sup>116,117</sup> (Fig. 9B). This innovative strategy enables the specific cleavage of RNA without the need for reverse transcription, thereby facilitating the detection of RNA mutations with single-base resolution. Additionally, Su *et al.* proposed a double-stranded body-specific nuclease (DSN-IEXPAR) method for detecting fusion transcripts<sup>118</sup> (Fig. 9C). In this approach, DNA probes are designed to recognize and hybridize with the target fusion transcript. Subsequently, the DSN nuclease cleaves DNA probes specifically within perfectly matched DNA/RNA double-

stranded regions. The cleaved and truncated DNA probe then triggers the downstream EXPAR.

Sun *et al.*'s pioneering work introduced the first application of a novel methylation-dependent restriction endonuclease, *GlaI*, coupled with EXPAR for site-specific DNA methylation detection<sup>119</sup> (Fig. 9D). *GlaI* exhibits exceptional selectivity, cleaving only methylated target sites. The newly exposed methylated DNA end fragments subsequently trigger EXPAR, enabling efficient signal amplification. This method achieves a remarkably low LOD of 200 aM for methylated DNA targets and boasts a rapid turnaround time, with the entire detection process of the *GlaI*-EXPAR system being completed within just two hours. Building upon this concept, An *et al.* established a fast and sensitive fluorescence sensing strategy for CpG methyltransferase (MTase) activity detection<sup>120</sup> (Fig. 9E). This method leverages the site-specific methylation capability of *M. sssI* MTase and the specific cleavage activity of *HpaII* to detect CpG MTase activity.

**Downstream specific recognition.** Lin *et al.* proposed a novel strategy for miRNA detection, employing a dual signal amplification approach that integrates mesophilic *Clostridium perfringens* Argonaute (CpAgo) downstream of the EXPAR.<sup>121</sup> This innovative strategy leverages EXPAR amplification fragments with a 5'-phosphate group as DNA guides. These guides enable CpAgo-programmed cleavage of detection probes in a second

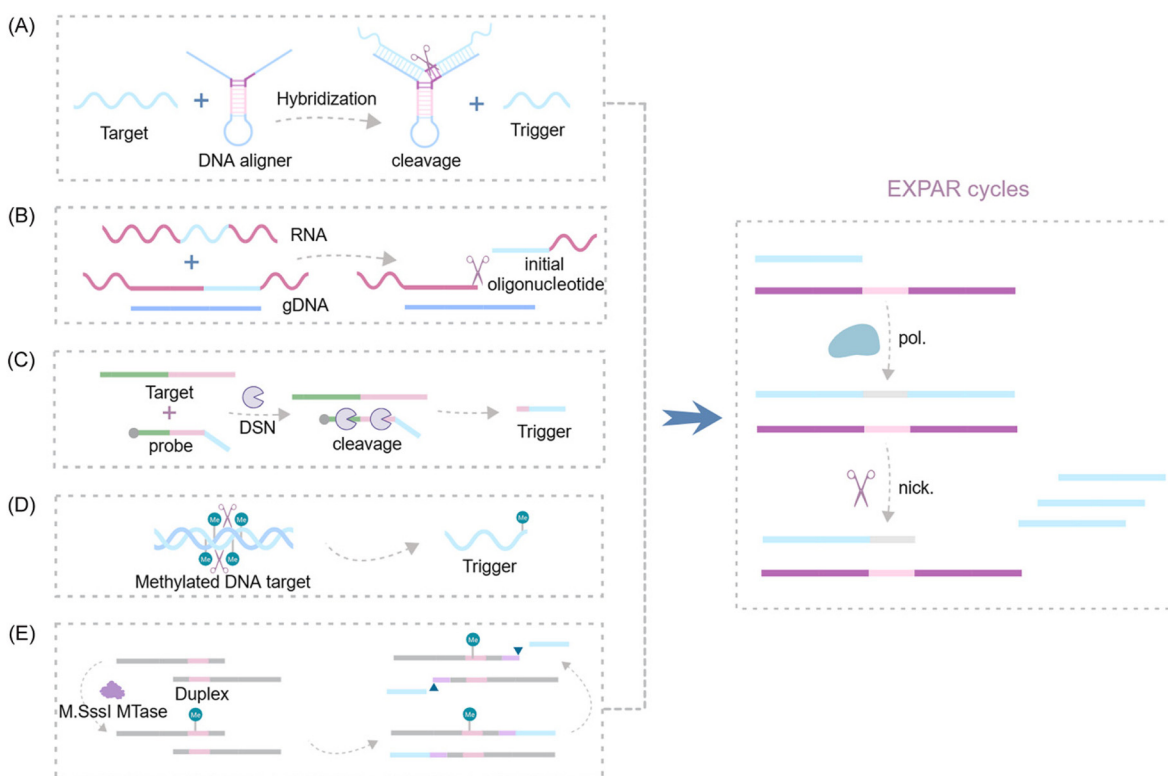


**Fig. 9** Schematic representation of nuclease-based approaches by upstream recognition. (A) Aligner-mediated cleavage-triggered EXPAR.<sup>25,115</sup> (B) Methods of nuclease-mediated RNA cleavage for triggering EXPAR.<sup>116,117</sup> (C) Detection of fusion transcripts based on a duplex-specific nuclease and EXPAR.<sup>118</sup> (D) A novel *GlaI*-assisted EXPAR assay (*GlaI*-EXPAR) to direct quantification of methylated DNA.<sup>119</sup> (E) A fluorescence strategy for detecting CpG MTase activity based on *HpaII*-assisted EXPAR.<sup>120</sup>





amplification stage. This two-step process achieves significant signal amplification for miRNA detection within a single reaction vessel. Notably, the CpAgo-based one-pot method demonstrates exceptional sensitivity, enabling the detection of miRNA targets as low as 1 zM within just 30 minutes. This approach holds considerable promise for both scientific research and clinical applications.

**Upstream and downstream specific recognition.** Zhang *et al.* developed a novel fluorescence-based assay for detecting DNA methyltransferase (MTase) by capitalizing on the inherent DNA damage repair mechanism<sup>122</sup> (Fig. 10A). Their approach leverages the cascade IAT guided by DNA damage repair. This method incorporates DpnI-mediated cleavage of methylated DNA substrates upstream of the EXPAR and exploits the dual functionality of Endo IV. Endo IV simultaneously participates in the EXPAR cycling system and cleaves signal probes downstream of EXPAR. This innovative strategy achieves a remark-

able detection limit of  $0.014 \text{ U mL}^{-1}$  for DNA adenine methylation (Dam) MTase.

Another study introduced Endo IV into the EXPAR strategy, establishing a novel approach for sensitive detection of transcription factors (TFs) based on bidirectional EXPAR with nucleic acid Endo IV-assisted signaling probe circular digestion<sup>123</sup> (Fig. 10B). This method leverages bidirectional amplification and Endo IV-mediated circular digestion of the signaling probe to achieve high sensitivity. Furthermore, Chen *et al.* developed a convenient fluorescence-based method for rapid and sensitive detection of Flap endonuclease 1 (FEN1)<sup>124</sup> (Fig. 10C). This strategy exploits the exponential amplification of a bi-enzymatic repair process coupled with a multi-terminal signal output. FEN1 initiates the process by cleaving a dual-branched substrate upstream, generating abundant ssDNA. Subsequently, the ssDNA hybridizes with downstream signal probes to form partially complementary dsDNA. Finally, T7

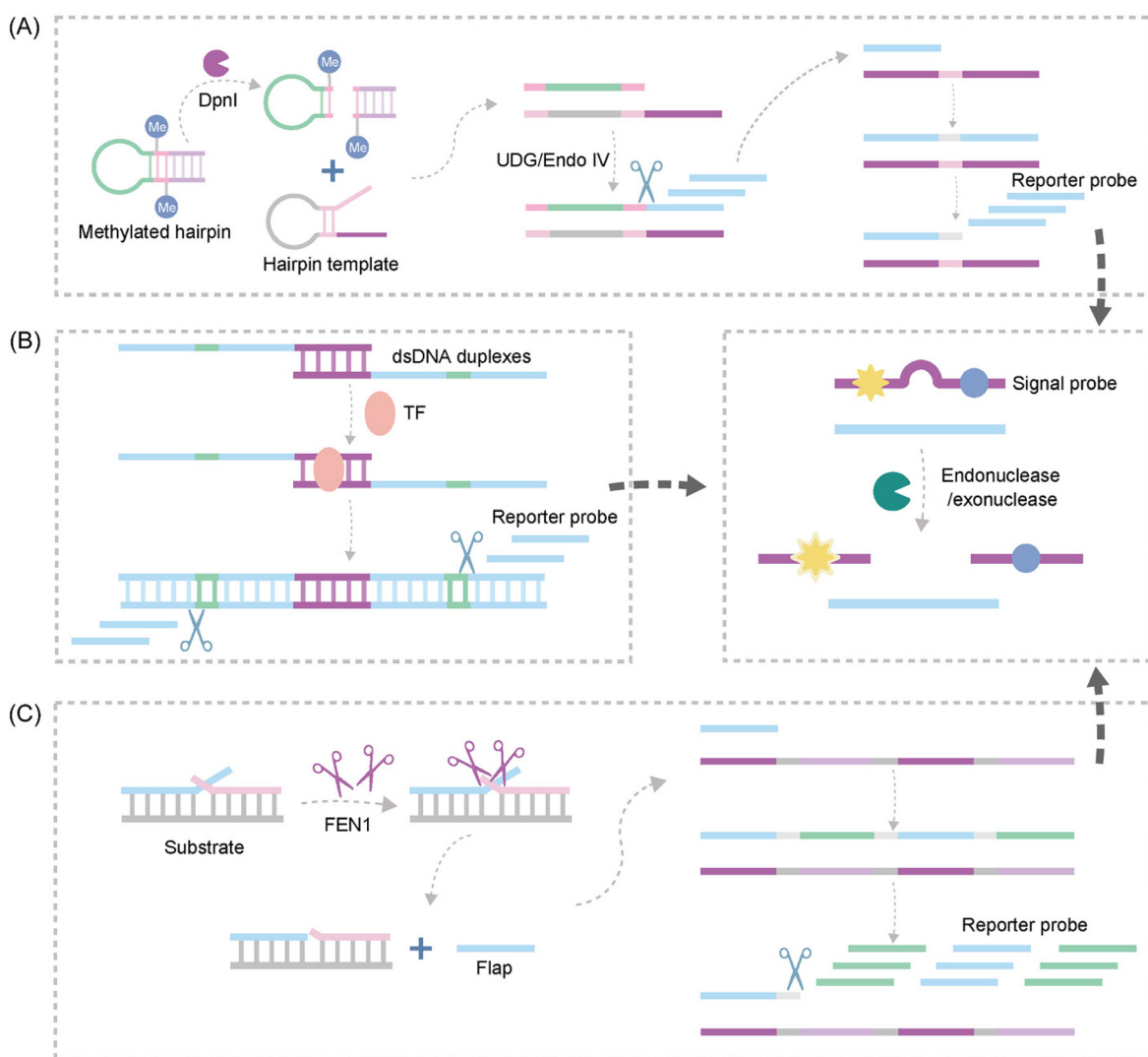


**Fig. 10** Schematic representation of nuclease-based approaches by upstream and downstream recognition. (A) DNA lesion repair-directed cascade EXPAR for detecting DNA Mtase.<sup>122</sup> (B) A new strategy to detect TFs based on bidirectional EXPAR and an Endo IV-assisted cycle.<sup>123</sup> (C) A fluorescence method for detecting FEN1 based on dual enzymatic repair EXPAR with multi-terminal signal output.<sup>124</sup>



exonuclease digests the signal probe on dsDNA, releasing a fluorescence signal.

**Enzyme-specific chemical modification.** Several researchers have capitalized on the inherent activation properties of enzymes to develop effective methods for detecting enzymatic activities. These methods often combine enzyme activation or deactivation with strategically designed sequences. For

instance, both Zhang and Chen exploited the bifunctional nature of T4 polynucleotide kinase phosphatase (T4 PNKP) – an enzyme that can phosphorylate the 5' hydroxyl group and remove the terminal 3' phosphate group – by employing EXPAR as a carrier to assay T4 PNKP activity.<sup>20,125</sup> Cheng *et al.* made a significant contribution by pioneering the integration of a lateral flow assay into EXPAR to visualize telomerase

**Table 1** Comparison of different EXPAR-based approaches

| Method                  | Type                               | Target                       | Dynamic range   | LOD   | Ref.                     |             |
|-------------------------|------------------------------------|------------------------------|---|---|--------------------------|-------------|
| Modified template       | STD-template                       | let-7a                       | 0.01 zmol–0.01 nmol   | 0.01 zmol                                   | 35                       |             |
|                         | SEXPAR-FISH                        | miR-27a                      | 1 fM–10 nM  | 1 fM  | 36                       |             |
|                         | cEXPAR                             | miR-21                       | N/A   | 1 ymol                                      | 38                       |             |
|                         | CoOOH, hexanediol phosphorothioate | miR-122                      | N/A   | 7.58 aM                                     | 39                       |             |
| CRISPR/Cas              | Cas9                               | ssDNA                        | 1 fM–1 nM   | 0.7 fM                                      | 29                       |             |
|                         |                                    | HLY DNA                      | 1 amol–10 fmol  | 0.82 amol                                   | 50                       |             |
|                         |                                    | ssDNA                        | 100 aM–1 nM   | 100 aM                                      | 51                       |             |
|                         |                                    | HER2                         | 1 fM–1 nM   | 437 aM                                      | 52                       |             |
|                         | Cas12a                             | Antibiotic-resistant genes   | 100 fM–1 nM   | 100 aM                                      | 53                       |             |
|                         |                                    | miR-27a                      | 100 aM–10 nM  | 90 aM                                       | 49                       |             |
|                         |                                    | SARS-CoV-2 RNA               | N/A   | 3.77 aM                                     | 57                       |             |
|                         |                                    | miRNAs-21                    | 1 pM–100 pM   | 103 fM                                      | 28                       |             |
|                         |                                    | miR-21                       | 1 μM–1 fM   | 1 fM  | 21                       |             |
|                         |                                    | p53                          | 500 aM–10 pM, 10 pM–1 nM                                      | 0.39 fM                                     | 58                       |             |
|                         | Cas13                              | Dam MTase                    | $2 \times 10^{-4}$ – $10 \text{ U mL}^{-1}$                   | $2 \times 10^{-4} \text{ U mL}^{-1}$        | 59                       |             |
|                         |                                    | CLDN11 methylation           | $3 \times 10^{-15}$ – $4.8 \times 10^{-14} \text{ M}$         | $1.25 \times 10^{-15} \text{ M}$            | 60                       |             |
|                         |                                    | miR-17                       | $1 \times 10^{-12}$ – $1 \times 10^{-15} \text{ M}$           | $1 \times 10^{-15} \text{ M}$               | 45                       |             |
|                         |                                    | Cas14a                       | CK-MB   | $3.55 \times 10^{-4}$ – $119.03 \text{ nM}$ | 0.355 pM                 | 65          |
| Aptamer                 | Aptamer                            | PDGF-BB                      | 0.1 pM–1 nM   | 52 fM                                       | 69                       |             |
|                         |                                    | Theophylline                 | 0.5–1000 μM   | 0.5 μM                                      | 70 and 71                |             |
|                         |                                    | Mycotoxin T-2                | 1 pg mL <sup>-1</sup> –100 ng mL <sup>-1</sup>                | 30 fg mL <sup>-1</sup>                      | 72                       |             |
|                         |                                    | <i>Cronobacter sakazakii</i> | N/A   | 2 cfu mL <sup>-1</sup>                      | 73                       |             |
| IATs                    | HCR                                | PDGF-BB                      | 10 fM–10 nM   | 4.9 fM                                      | 74                       |             |
|                         |                                    | Cu <sup>2+</sup>             | N/A   | 10 pM                                       | 84                       |             |
|                         |                                    | E2                           | 0.4–800 pg mL <sup>-1</sup>                                   | 0.37 pg mL <sup>-1</sup>                    | 85                       |             |
|                         |                                    | BRCA1                        | 0.1 fM–100 pM   | 74.48 aM                                    | 83                       |             |
| MNCs                    | AuNP                               | NGF-β                        | 1 fM–100 nM   | 0.74 fM                                     | 90                       |             |
|                         |                                    | ALP                          | $1.0 \times 10^{-9}$ – $1.0 \times 10^{-4} \text{ U μL}^{-1}$ | $2.0 \times 10^{-10} \text{ U μL}^{-1}$     | 93                       |             |
|                         |                                    | DNA glycosylase              | 0.16–8.0 U m <sup>-1</sup>                                    | 0.14 U m <sup>-1</sup>                      | 94                       |             |
|                         |                                    | miRNAs                       | 1 aM–1 nM   | 4.176 aM                                    | 101                      |             |
| Enzyme                  | AgNC                               | miR-21                       | 0.75–10 000 fM  | 0.23 fM                                     | 102                      |             |
|                         |                                    | Ricin                        | 10 pM–50 nM   | 2.25 pM                                     | 103                      |             |
|                         |                                    | miRNAs-141                   | 1–500 fM  | 0.87 fM                                     | 106                      |             |
|                         |                                    | HIV-DNA                      | $1 \times 10^{-13}$ – $1 \times 10^{-10} \text{ M}$           | 4.7 fM                                      | 112                      |             |
|                         | DNAzyme                            | Pb <sup>2+</sup>             | 0.1–5 nM  | 95 pM                                       | 113                      |             |
|                         |                                    | FTO                          | 0.2 pM–25 nM  | 63.1 fM                                     | 114                      |             |
|                         |                                    | ssDNA                        | N/A   | 1 pM  | 25 and 115               |             |
|                         |                                    | TtAgo                        | SARS-CoV-2 N gene   | 1 aM–10 nM                                  | 1 aM                     | 116 and 117 |
|                         |                                    | RNase H                      | BRAF mRNA V600E   | 1 fM–100 pM                                 | 1 fM                     | 116 and 117 |
|                         |                                    | Duplex-specific nuclease     | Fusion transcript   | 100 fM–300 pM                               | 100 fM                   | 118         |
|                         |                                    | GlaI                         | Septin 9 gene   | 200 aM–200 pM                               | 200 aM                   | 119         |
|                         |                                    | HpaII                        | CpG MTase   | 0.125–8 U mL <sup>-1</sup>                  | 0.034 U mL <sup>-1</sup> | 120         |
|                         |                                    | CpAgo                        | miRNAs  | 1 zM–1 nM                                   | 1 zM                     | 121         |
|                         |                                    | Endo IV/DpnI                 | DNA MTase   | 0.02–10 U mL <sup>-1</sup>                  | 0.014 U mL <sup>-1</sup> | 122         |
| Others                  | Endo IV                            | TF                           | $6.4 \times 10^{-14}$ – $8 \times 10^{-7} \text{ M}$          | $1.29 \times 10^{-14} \text{ M}$            | 123                      |             |
|                         | T7 exonuclease                     | FEN1                         | N/A   | $9.7 \times 10^{-3} \text{ U mL}^{-1}$      | 124                      |             |
|                         | T4 PNKP                            | T4 PNKP                      | $5 \times 10^{-6}$ – $0.005 \text{ U mL}^{-1}$                | $1.5 \times 10^{-6} \text{ U mL}^{-1}$      | 20 and 125               |             |
|                         | T4 PNKP                            | T4 PNKP                      | 0.001–0.01 U mL <sup>-1</sup>                                 | $7.9 \times 10^{-4} \text{ U mL}^{-1}$      | 20 and 125               |             |
|                         | NEase                              | ssDNA                        | 25 fmol–2.5 amol  | 1.37 amol                                   |                          |             |
|                         | Telomerase                         | Telomerase                   | N/A   | 1 pM  | 126                      |             |
|                         | pH                                 | PDGF-BB, PDGF-BB             | 10 fM–100 pM  | 9.6 fM                                      | 127                      |             |
|                         | P-HP                               | ssDNA                        | 10 pM–300 nM  | 10 pM                                       | 128                      |             |
| HP                      | let7-a                             | 1–10 <sup>10</sup> copies    | 1 copies  | 129   |                          |             |
| MIL                     | let7 family                        | N/A                          | 10 aM   | 130   |                          |             |
| RTF                     | SARS-CoV-2 RNA                     | N/A                          | 7.25 copies per μL  | 56  |                          |             |
| Bipedal 3-D DNA walkers | miR-21                             | 10 fM–5 nM                   | 5.2 fM  | 22  |                          |             |
| MALDI-TOF MS            | miRNAs                             | N/A                          | 1 amol  | 131   |                          |             |
| Disposable sensor chip  | miRNAs-223                         | 100 fM–100 nM                | N/A   | 132   |                          |             |



activity. This novel approach, termed the lateral flow readout-EXPAR (LFR-EXPAR) assay, leverages the telomerase extension product to initiate EXPAR.<sup>126</sup> The resulting triggers then hybridize with the reporter gene, forming a recognition site for a downstream enzymatic cleavage event. Subsequently, the degradation of the reporter gene strand by the incision enzyme can be visualized using standard lateral flow test paper, enabling detection with the naked eye.

Integrating nucleases into the EXPAR system offers several advantages for target detection. Firstly, upstream endonucleases or exonucleases can be employed for specific recognition and cleavage of the target sequence. This cleavage event releases ssDNA that can trigger EXPAR amplification. This strategy not only enhances the reaction's specificity but also expands the range of detectable targets amenable for analysis. Secondly, the amplified products of EXPAR can hybridize with signal probes, creating recognition sites for downstream cleavage enzymes. Activation of these cleavage enzymes triggers the release of a signal. This signal conversion, achieved by detecting probe signals, effectively reduces non-specific background signals. Thirdly, strategically designed chemical modifications can be employed to harness the catalytic activity of enzymes to initiate EXPAR and facilitate subsequent detection. However, limitations associated with cleavage enzymes pose challenges to the overall amplification cascade within the EXPAR system. These limitations include the restricted availability of suitable enzymes, their temperature sensitivity, and the limited repertoire of recognition sites they can target. Consequently, these factors can constrain the extent of enzymatic amplification achievable within the EXPAR cascade.

## EXPAR-based assays incorporating other methods

Beyond the general optimizations of EXPAR techniques, several innovative applications have emerged for detecting small molecule markers using EXPAR technology. For example, Mao *et al.* introduced a pH-dependent immunoanalytical platform that leverages immunotriggered EXPAR to convert the immune response of target detection into measurable pH variations.<sup>127</sup> This approach facilitates protein detection through the utilization of a colorimetric pH indicator. Another advancement came from Yan *et al.*, who constructed a novel multifunctional hairpin probe (P-HP) incorporating palindromic fragments for a symmetric EXPAR (S-EXPAR) method.<sup>128</sup> This design significantly reduces nonspecific amplification in the EXPAR. Similarly, Kim *et al.* developed a target-inducible strand amplification reaction for detecting target microRNAs (miRNAs) by employing cleverly designed, interrelated reaction pathways<sup>129</sup> (Table 1).

Several innovative strategies have further expanded the capabilities of the EXPAR system. Emaus *et al.* investigated using hydrophobic magnetic ionic liquids (MILs) within the EXPAR buffer. Interestingly, they found that MILs can reduce background signals caused by nonspecific amplification while

simultaneously increasing the reaction rate.<sup>130</sup> Building upon previous work, Carter *et al.* successfully combined EXPAR with isothermal reverse transcription (RTF) to create the RTF-EXPAR assay.<sup>56</sup> This assay demonstrates high accuracy, achieving the detection of 7.25 copies per  $\mu\text{L}$  of SARS-CoV-2 RNA within a rapid 10-minute timeframe. In another advancement, Yang *et al.* constructed a novel bipedal 3D DNA walker sensor that integrates EXPAR in solution. This innovative design combines EXPAR with an enzymatic cleavage reaction performed on particles, enabling highly sensitive and selective detection of miRNAs.<sup>22</sup> Focusing on label-free and multiplexed miRNA detection, Han *et al.* coupled EXPAR with matrix-assisted laser desorption/ionization time-of-flight mass spectrometry (MALDI-TOF MS).<sup>131</sup> This approach utilizes EXPAR to generate short products, facilitating the simultaneous detection of multiple miRNAs without the need for additional labels. Further advancement in miRNA detection came from Qian *et al.*, who developed a chip-based exosomal miRNA amplification and detection system.<sup>132</sup> This microfluidic platform integrates both exosomal miRNA extraction and detection, enabling rapid analysis of these biomarkers and paving the way for real-time liquid biopsy applications.

## Conclusion and perspectives

This review has delineated the significant advancements achieved in EXPAR technology for sensor development over the past five years. A key focus of these assays has been to address the challenges associated with non-specific amplification, a common hurdle in conventional EXPAR systems primarily arising from template self-priming. Additionally, researchers have sought to overcome limitations in sensitivity observed in many IATs. To achieve these goals, a diverse array of strategies have been implemented, leveraging various signal amplification mechanisms such as fluorescence, colorimetry, electrochemistry, and chemiluminescence. These strategies are often integrated with diverse molecular technological platforms, including CRISPR/Cas systems, aptamers, metal nanoparticles, other IATs, and enzymes. This combined approach has led to the development of highly sensitive and specific sensors for a wide range of analytes.

EXPAR offers several distinct advantages compared to other well-established IATs. Firstly, EXPAR exhibits exceptional amplification efficiency within the category of exponential isothermal amplification. It can achieve a remarkable  $10^8$ -fold increase in target abundance within just a few minutes, which is comparable to the amplification efficiency of the currently burgeoning isothermal amplification techniques such as LAMP and RPA.<sup>9,18,24,133–135</sup> Secondly, the experimental design of EXPAR is noteworthy for its simplicity. In contrast to LAMP, which necessitates the design of multiple primers for specific regions within the target sequence, EXPAR only requires the design of a single amplification template. For instance, LAMP-based miRNA detection often involves intricate probe design due to the LAMP template's inclusion of 4 to 6 predefined



sequences for stem-loop formation. Additionally, the coordinated hybridization and extension of multiple primers along the extended LAMP template can potentially compromise the sensitivity of this strategy.<sup>136</sup> EXPAR, on the other hand, streamlines the reaction system compared to RPA-based methods by eliminating the need for multiple enzymes. This simplification allows EXPAR to maintain reaction stability even in complex environments.<sup>9</sup> One of the most prominent applications of EXPAR-based biosensing systems lies in the detection of miRNAs. Due to their small molecular weight, short sequences, and high degree of homology, direct and precise detection of miRNAs remains a challenge. Currently, EXPAR and RCA are the primary methods employed for the detection of short DNA or RNA strands.<sup>137</sup> However, RCA necessitates a circular DNA template for amplification, while EXPAR can achieve miRNA amplification using a simpler ssDNA template. Notably, other IATs are primarily suited for amplifying DNA or messenger RNA (mRNA). When applied to miRNA detection, these methods often involve more cumbersome procedures, limiting their applicability in this context.

Despite the advancements in EXPAR biointerfacing strategies, further research is necessary to broaden its applicability and clinical utility. (1) Owing to its concise sequence trigger, the majority of innovative sensing methodologies devised for EXPAR are tailored for miRNA detection. This implies that there are still constraints regarding the detection of alternative molecular biomarkers using EXPAR. Consequently, forthcoming EXPAR-based biosensing strategies ought to extend the spectrum of detectable targets. (2) Live cell bioimaging represents a promising direction for IATs, with growing interest in their application for this purpose. However, the optimal reaction temperature for EXPAR, which is approximately 55 °C, currently impedes its utility in live-cell studies. Consequently, researchers must investigate the feasibility of low-temperature EXPAR to unlock its potential in this field.<sup>88,138</sup> (3) The integration of novel reaction components in some EXPAR designs can increase system complexity and instability, potentially leading to false-positive results. Future strategies should prioritize streamlined fabrication processes and minimal inclusion of elements that could compromise reaction stability, ultimately enhancing detection accuracy. (4) The critical role of the EXPAR template sequence design in generating amplification products presents a challenge. Meticulous design is needed to prevent both template self-dimerization and non-specific target-template binding. This limitation hampers the generalizability of EXPAR-based biosensing strategies, underscoring the need for future strategies to prioritize method generalization. (5) While many EXPAR-based studies have focused on single biomarkers, diseases frequently involve multiple dys-regulated biomarkers. Multi-target detection strategies hold promise for providing more comprehensive biological insights, leading to more precise diagnoses and treatment strategies. (6) EXPAR-based technology lags behind other IATs in terms of commercialization. Although the RTF-EXPAR technology developed by the University of Birmingham<sup>56</sup> and licensed to Innova Medical Group exemplifies its commercial potential,

mature assay kits have not been launched yet. This likely stems from EXPAR's inherent high background signal issues that hinder its commercial viability. However, recent research efforts, fueled by the COVID-19 pandemic and advancements in molecular diagnostics like CRISPR, focus on reducing non-specific interference in EXPAR detection. Researchers are working on meticulously integrating highly specific signal amplification techniques, which may pave the way for EXPAR's commercialization.

Despite facing numerous challenges, isothermal amplification-based biosensing methodologies are experiencing rapid advancement, marked by the introduction of groundbreaking ideas and breakthroughs. We can expect the continued development of EXPAR-based biosensors with enhanced sensitivity, user-friendliness, and adaptability, offering significant advantages for POCT, clinical diagnostics, and disease management.

## Author contributions

Xinyi Ou: conceptualization, writing – original draft, and visualization; Kunxiang Li: writing – review & editing; Miao Liu: visualization; Jiajun Song: visualization; Zhihua Zuo: writing – review & editing; Yongcan Guo: conceptualization, writing – review & editing, and visualization.

## Data availability

Data sharing is not applicable to this article as no new data were created or analyzed in this study.

## Conflicts of interest

There are no conflicts to declare.

## Acknowledgements

This work was supported by the Applied Basic Research Foundation of Sichuan Provincial Science and Technology Department (No. 2021JY0240), Sichuan Science and Technology Program (No. 2022YFS0623 and No. 2023ZYD0287), Luzhou Municipal People's Government and Southwest Medical University (No. 2021LZXNYD-D01), Health Commission of Sichuan Province (No. 21ZD006), Medical Research Project of Sichuan Medical Association (No. S21038), and Southwest Medical University (No. 2023ZYQJ01).

## References

- 1 L. Xu, J. Duan, J. Chen, S. Ding and W. Cheng, *Anal. Chim. Acta*, 2021, **1148**, 238187.
- 2 L. S. Pessoa, M. Heringer and V. P. Ferrer, *Crit. Rev. Oncol. Hematol.*, 2020, **155**, 103109.





- 3 L. B. S. Aulin, D. W. de Lange, M. A. A. Saleh, P. H. van der Graaf, S. Völler and J. G. C. van Hasselt, *Clin. Pharmacol. Ther.*, 2021, **110**, 346–360.
- 4 C. Jin, Z. Wu, J. H. Molinski, J. Zhou, Y. Ren and J. X. J. Zhang, *Mater. Today Bio*, 2022, **14**, 100263.
- 5 M. Luo, F. Lan, W. Li, S. Chen, L. Zhang, B. Situ, B. Li, C. Liu, W. Pan, Z. Gao, Y. Zhang and L. Zheng, *Anal. Chim. Acta*, 2023, **1283**, 341824.
- 6 R. Liu, X. Ye and T. Cui, *Research*, 2020, **2020**, 7949037.
- 7 A. N. Simpkins, M. Janowski, H. S. Oz, J. Roberts, G. Bix, S. Doré and A. M. Stowe, *Transl. Stroke Res.*, 2020, **11**, 615–627.
- 8 R. K. Saiki, D. H. Gelfand, S. Stoffel, S. J. Scharf, R. Higuchi, G. T. Horn, K. B. Mullis and H. A. Erlich, *Science*, 1988, **239**, 487–491.
- 9 H. Qi, S. Yue, S. Bi, C. Ding and W. Song, *Biosens. Bioelectron.*, 2018, **110**, 207–217.
- 10 J. W. Park, *Biosensors*, 2022, **12**, 857.
- 11 C. Suther, S. Stoufer, Y. Zhou and M. D. Moore, *Front. Microbiol.*, 2022, **13**, 841875.
- 12 T. Notomi, H. Okayama, H. Masubuchi, T. Yonekawa, K. Watanabe, N. Amino and T. Hase, *Nucleic Acids Res.*, 2000, **28**, E63.
- 13 I. M. Lobato and C. K. O'Sullivan, *TrAC, Trends Anal. Chem.*, 2018, **98**, 19–35.
- 14 M. Vincent, Y. Xu and H. Kong, *EMBO Rep.*, 2004, **5**, 795–800.
- 15 H. Li, W. Song, H. Li, J. Cui, Y. Xie, B. Wu and R. Chen, *Analyst*, 2023, **148**, 3708–3718.
- 16 G. M. van der Vliet, R. A. Schukking, B. van Gemen, P. Schepers and P. R. Klatser, *J. Gen. Microbiol.*, 1993, **139**, 2423–2429.
- 17 C. Qian, R. Wang, H. Wu, F. Ji and J. Wu, *Anal. Chim. Acta*, 2019, **1050**, 1–15.
- 18 C. Zhang, T. Belwal, Z. Luo, B. Su and X. Lin, *Small*, 2022, **18**, e2102711.
- 19 Y. Xu, D. Li, W. Cheng, R. Hu, Y. Sang, Y. Yin, S. Ding and H. Ju, *Anal. Chim. Acta*, 2016, **936**, 229–235.
- 20 H. Chen, Z. Wang, X. Chen, K. Lou, A. Sheng, T. Chen, G. Chen and J. Zhang, *Analyst*, 2019, **144**, 1955–1959.
- 21 H. Wei, S. Bu, Z. Wang, H. Zhou, X. Li, J. Wei, X. He and J. Wan, *ACS Omega*, 2022, **7**, 35515–35522.
- 22 L. Yang, J. Fang, J. Li, X. Ou, L. Zhang, Y. Wang, Z. Weng and G. Xie, *Anal. Chim. Acta*, 2021, **1143**, 157–165.
- 23 J. Van Ness, L. K. Van Ness and D. J. Galas, *Proc. Natl. Acad. Sci. U. S. A.*, 2003, **100**, 4504–4509.
- 24 E. A. Pumford, J. Lu, I. Spaczai, M. E. Prasetyo, E. M. Zheng, H. Zhang and D. T. Kamei, *Biosens. Bioelectron.*, 2020, **170**, 112674.
- 25 W. Wu, H. Fan, X. Lian, J. Zhou and T. Zhang, *Talanta*, 2018, **185**, 141–145.
- 26 G. Urtel, M. Van Der Hofstadt, J. C. Galas and A. Estevez-Torres, *Biochemistry*, 2019, **58**, 2675–2681.
- 27 M. S. Reid, R. E. Paliwoda, H. Zhang and X. C. Le, *Anal. Chem.*, 2018, **90**, 11033–11039.
- 28 C. Niu, J. Liu, X. Xing and C. Zhang, *Anal. Chim. Acta*, 2023, **1251**, 340998.
- 29 J. Mao, S. Tang, S. Liang, W. Pan, Y. Kang, J. Cheng, D. Yu, J. Chen, J. Lou, H. Zhao and J. Zhou, *Anal. Methods*, 2021, **13**, 3947–3953.
- 30 J. Chen, X. Zhou, Y. Ma, X. Lin, Z. Dai and X. Zou, *Nucleic Acids Res.*, 2016, **44**, e130.
- 31 M. S. Reid, X. C. Le and H. Zhang, *Angew. Chem., Int. Ed.*, 2018, **57**, 11856–11866.
- 32 H. Jia, Z. Li, C. Liu and Y. Cheng, *Angew. Chem., Int. Ed.*, 2010, **49**, 5498–5501.
- 33 X. Zhang, C. Liu, L. Sun, X. Duan and Z. Li, *Chem. Sci.*, 2015, **6**, 6213–6218.
- 34 Y. Zhang and C.-Y. Zhang, *Anal. Chem.*, 2012, **84**, 224–231.
- 35 J. Chen, T. An, Y. Ma, B. Situ, D. Chen, Y. Xu, L. Zhang, Z. Dai and X. Zou, *Anal. Chem.*, 2018, **90**, 859–865.
- 36 J. Chen, W. Yin, Y. Ma, H. Yang, Y. Zhang, M. Xu, X. Zheng, Z. Dai and X. Zou, *Chem. Commun.*, 2018, **54**, 13981–13984.
- 37 W. Yin, J. Chen, H. Yang, Y. Zhang, Z. Dai and X. Zou, *Chem. Commun.*, 2019, **55**, 11251–11254.
- 38 X. M. Qu, X. D. Ren, N. Su, X. G. Sun, S. L. Deng, W. P. Lu and Q. Huang, *Mol. Biol. Rep.*, 2023, **50**, 3653–3659.
- 39 M. P. Trinh, J. G. Carballo, G. B. Adkins, K. Guo and W. Zhong, *Anal. Bioanal. Chem.*, 2020, **412**, 2399–2412.
- 40 C. Jiang, Y. Li, X. Zhang, Y. Shan, C. Ma and C. Shi, *Anal. Lett.*, 2024, 1–15, DOI: [10.1080/00032719.2024.2326984](https://doi.org/10.1080/00032719.2024.2326984).
- 41 Q. Lin, X. Ye, H. Chen, X. Fang, H. Chen and J. Kong, *Anal. Chem.*, 2024, **96**, 620–623.
- 42 M. Wang, R. Zhang and J. Li, *Biosens. Bioelectron.*, 2020, **165**, 112430.
- 43 H. Nishimasu, F. A. Ran, P. D. Hsu, S. Konermann, S. I. Shehata, N. Dohmae, R. Ishitani, F. Zhang and O. Nureki, *Cell*, 2014, **156**, 935–949.
- 44 W. Y. Wu, J. H. G. Lebbink, R. Kanaar, N. Geijsen and J. van der Oost, *Nat. Chem. Biol.*, 2018, **14**, 642–651.
- 45 T. Zhou, R. Huang, M. Huang, J. Shen, Y. Shan and D. Xing, *Adv. Sci.*, 2020, **7**, 1903661.
- 46 J. E. van Dongen, J. T. W. Berendsen, R. D. M. Steenbergen, R. M. F. Wolthuis, J. C. T. Eijkel and L. I. Segerink, *Biosens. Bioelectron.*, 2020, **166**, 112445.
- 47 R. Sundaresan, H. P. Parameshwaran, S. D. Yogesha, M. W. Keilbarth and R. Rajan, *Cell Rep.*, 2017, **21**, 3728–3739.
- 48 O. O. Abudayyeh, J. S. Gootenberg, S. Konermann, J. Joung, I. M. Slaymaker, D. B. Cox, S. Shmakov, K. S. Makarova, E. Semenova, L. Minakhin, K. Severinov, A. Regev, E. S. Lander, E. V. Koonin and F. Zhang, *Science*, 2016, **353**, aaf5573.
- 49 Y. Yang, J. Yang, F. Gong, P. Zuo, Z. Tan, J. Li, C. Xie, X. Ji, W. Li and Z. He, *Sens. Actuators, B*, 2022, **367**, 132158.
- 50 M. Huang, X. Zhou, H. Wang and D. Xing, *Anal. Chem.*, 2018, **90**, 2193–2200.
- 51 X. Wang, X. Chen, C. Chu, Y. Deng, M. Yang, D. Huo, F. Xu, C. Hou and J. Lv, *Talanta*, 2021, **233**, 122554.



- 52 J. Song, S. Kim, H. Y. Kim, K. H. Hur, Y. Kim and H. G. Park, *Nanoscale*, 2021, **13**, 7193–7201.
- 53 K. Qin, P. Zhang and Z. Li, *Talanta*, 2023, **253**, 124045.
- 54 W. Feng, A. M. Newbigging, J. Tao, Y. Cao, H. Peng, C. Le, J. Wu, B. Pang, J. Li, D. L. Tyrrell, H. Zhang and X. C. Le, *Chem. Sci.*, 2021, **12**, 4683–4698.
- 55 B. Paul and G. Montoya, *Biomed. J.*, 2020, **43**, 8–17.
- 56 J. G. Carter, L. Orueta Iturbe, J. H. A. Duprey, I. R. Carter, C. D. Southern, M. Rana, C. M. Whalley, A. Bosworth, A. D. Beggs, M. R. Hicks, J. H. R. Tucker and T. R. Dafforn, *Proc. Natl. Acad. Sci. U. S. A.*, 2021, **118**, e2100347118.
- 57 X. M. Hang, H. Y. Wang, P. F. Liu, K. R. Zhao and L. Wang, *Biosens. Bioelectron.*, 2022, **216**, 114683.
- 58 S. Zhou, L. Deng, J. Dong, P. Lu, N. Qi, Z. Huang, M. Yang, D. Huo and C. Hou, *Mikrochim. Acta*, 2023, **190**, 113.
- 59 H. Sun, S. Zhou, Y. Liu, P. Lu, N. Qi, G. Wang, M. Yang, D. Huo and C. Hou, *Anal. Chim. Acta*, 2023, **1239**, 340732.
- 60 Q. Wu, X. Xiang, Y. Yuan, Y. Yu, M. Chen, J. Long, T. Xiang and X. Yang, *Sens. Actuators, B*, 2023, **385**, 133675.
- 61 D. Shihong Gao, X. Zhu and B. Lu, *J. Med. Virol.*, 2021, **93**, 4198–4204.
- 62 L. Yin, S. Man, S. Ye, G. Liu and L. Ma, *Biosens. Bioelectron.*, 2021, **193**, 113541.
- 63 G. Aquino-Jarquín, *Nanomedicine*, 2019, **18**, 428–431.
- 64 M. Z. Khan, S. Haider, S. Mansoor and I. Amin, *Trends Biotechnol.*, 2019, **37**, 800–804.
- 65 M. Chen, J. Zhang, Y. Peng, J. Bai, S. Li, D. Han, S. Ren, K. Qin, H. Zhou, T. Han, Y. Wang and Z. Gao, *Biosens. Bioelectron.*, 2022, **218**, 114792.
- 66 L. Wu, Y. Wang, X. Xu, Y. Liu, B. Lin, M. Zhang, J. Zhang, S. Wan, C. Yang and W. Tan, *Chem. Rev.*, 2021, **121**, 12035–12105.
- 67 R. Xu, Y. Cheng, X. Li, Z. Zhang, M. Zhu, X. Qi, L. Chen and L. Han, *Anal. Chim. Acta*, 2022, **1209**, 339893.
- 68 X. Zhou, Q. Zhu and Y. Yang, *Biosens. Bioelectron.*, 2020, **165**, 112422.
- 69 Y. Yu, G. Su, H. Zhu, Q. Zhu, Y. Chen, B. Xu, Y. Li and W. Zhang, *Int. J. Nanomed.*, 2017, **12**, 5903–5914.
- 70 A. M. Liao, W. Pan, J. C. Benson, A. D. Wong, B. J. Rose and G. T. Caltagirone, *Biochemistry*, 2018, **57**, 5117–5126.
- 71 A. M. Liao, T. T. T. Thoa and G. T. Caltagirone, *J. Visualized Exp.*, 2022, **188**, e64342.
- 72 M. Zhang, Y. Wang, S. Yuan, X. Sun, B. Huo, J. Bai, Y. Peng, B. Ning, B. Liu and Z. Gao, *Mikrochim. Acta*, 2019, **186**, 219.
- 73 X. Xu, L. Zhu, X. Wang, X. Lan, H. Chu, H. Tian and W. Xu, *Appl. Microbiol. Biotechnol.*, 2022, **106**, 4287–4296.
- 74 J. Chen, Y. Zhang, B. P. Xie, B. Sun, W. J. Duan, M. M. Li, J. X. Chen, Z. Dai and X. Zou, *Talanta*, 2021, **225**, 121980.
- 75 C. Zhang, J. Chen, R. Sun, Z. Huang, Z. Luo, C. Zhou, M. Wu, Y. Duan and Y. Li, *ACS Sens.*, 2020, **5**, 2977–3000.
- 76 Z. Zeng, R. Zhou, R. Sun, X. Zhang, D. Zhang, Q. Zhu and C. Chen, *Anal. Chim. Acta*, 2022, **1220**, 340048.
- 77 H. Sun, F. Yao, Z. Su and X. F. Kang, *Biosens. Bioelectron.*, 2020, **150**, 111906.
- 78 H. Xu, S. Zhang, T. Zhang, W. Huang, Y. Dai, R. Zheng and G. Wu, *Talanta*, 2022, **237**, 122967.
- 79 Y. Liu, S. Zhou, H. Sun, J. Dong, L. Deng, N. Qi, Y. Wang, D. Huo and C. Hou, *Anal. Chim. Acta*, 2022, **1215**, 339973.
- 80 J. Liu, Y. Zhang, H. Xie, L. Zhao, L. Zheng and H. Ye, *Small*, 2019, **15**, e1902989.
- 81 R. Zhou, Z. Zeng, R. Sun, W. Liu, Q. Zhu, X. Zhang and C. Chen, *Analyst*, 2021, **146**, 7087–7103.
- 82 Z. Zeng, R. Zhou, R. Sun, X. Zhang, Z. Cheng, C. Chen and Q. Zhu, *Biosens. Bioelectron.*, 2020, **173**, 112814.
- 83 Z. Tang, W. Zhao, Y. Sun, Y. Deng, J. Bao, C. Qiu, X. Xiao, Y. Xu, Z. Xie, J. Cai, X. Chen, M. Lin, G. Xu, Z. Chen and L. Yu, *Langmuir*, 2022, **38**, 12050–12057.
- 84 W. Xu, L. Zhu, X. Shao, K. Huang and Y. Luo, *Biosens. Bioelectron.*, 2018, **120**, 168–174.
- 85 Y. Wang, X. Zhao, M. Zhang, X. Sun, J. Bai, Y. Peng, S. Li, D. Han, S. Ren, J. Wang, T. Han, Y. Gao, B. Ning and Z. Gao, *Anal. Chim. Acta*, 2020, **1116**, 1–8.
- 86 J. Wang, Y. Sun, C. Lau and J. Lu, *Anal. Bioanal. Chem.*, 2020, **412**, 3019–3027.
- 87 W. Dai, J. Zhang, X. Meng, J. He, K. Zhang, Y. Cao, D. Wang, H. Dong and X. Zhang, *Theranostics*, 2018, **8**, 2646–2656.
- 88 Z. Tian, C. Zhou, C. Zhang, M. Wu, Y. Duan and Y. Li, *J. Mater. Chem. B*, 2022, **10**, 5303–5322.
- 89 X. Liu, X. Zhou, X. Xia and H. Xiang, *Anal. Chim. Acta*, 2020, **1096**, 159–165.
- 90 Z. Tang, W. Zhao, Y. Deng, Y. Sun, C. Qiu, B. Wu, J. Bao, Z. Chen and L. Yu, *Analyst*, 2022, **147**, 1709–1715.
- 91 H. Xu, H. Niu, J. Liu, Y. Zhang, H. Yin, D. Liu, Z. Jiang, S. Yu and Z. S. Wu, *Talanta*, 2020, **219**, 121295.
- 92 H. Xu, F. Yang, D. Chen, W. Ye, G. Xue and L. Jia, *iScience*, 2023, **26**, 106331.
- 93 L. J. Wang, Z. Y. Wang and C. Y. Zhang, *Analyst*, 2018, **143**, 4606–4613.
- 94 H. Zhang, F. Li, L. Wang, S. Shao, H. Chen and X. Chen, *Talanta*, 2020, **220**, 121422.
- 95 S. Han, Y. Zhao, Z. Zhang and G. Xu, *Molecules*, 2020, **25**, 5208.
- 96 M. V. Romeo, E. Lopez-Martinez, J. Berganza-Granda, F. Goni-de-Cerio and A. L. Cortajarena, *Nanoscale Adv.*, 2021, **3**, 1331–1341.
- 97 Y. Zhao, H. Zhou, S. Zhang and J. Xu, *Methods Appl. Fluoresc.*, 2019, **8**, 012001.
- 98 X. Lin, L. Zou, W. Lan, C. Liang, Y. Yin, J. Liang, Y. Zhou and J. Wang, *Dalton Trans.*, 2021, **51**, 27–39.
- 99 Z. He, T. Shu, L. Su and X. Zhang, *Molecules*, 2019, **24**, 3045.
- 100 Y. Seetang-Nun, W. Jaroenram, S. Sriurairatana, R. Suebsing and W. Kiatpathomchai, *Mol. Cell. Probes*, 2013, **27**, 71–79.
- 101 J. Jiang, B. Zhang, C. Zhang and Y. Guan, *Int. J. Mol. Sci.*, 2018, **19**, 3374.



- 102 S. Wei, G. Chen, X. Jia, X. Mao, T. Chen, D. Mao, W. Zhang and W. Xiong, *Anal. Chim. Acta*, 2020, **1095**, 179–184.
- 103 X. Sun, W. Wang, Y. Chai, Z. Zheng, Y. Wang, J. Bi, Q. Wang, Y. Hu and Z. Gao, *Analyst*, 2023, **148**, 690–699.
- 104 Z. Yuan, Y. C. Chen, H. W. Li and H. T. Chang, *Chem. Commun.*, 2014, **50**, 9800–9815.
- 105 S. Y. New, S. T. Lee and X. D. Su, *Nanoscale*, 2016, **8**, 17729–17746.
- 106 H. Wu, J. Wu, Y. Liu, H. Wang and P. Zou, *Mikrochim. Acta*, 2019, **186**, 715.
- 107 H. Yang, Y. Peng, M. Xu, S. Xu and Y. Zhou, *Crit. Rev. Anal. Chem.*, 2023, **53**, 161–176.
- 108 N. Wang, L. Song, T. Deng and J. Li, *Anal. Chim. Acta*, 2020, **1140**, 69–77.
- 109 J. Li, K. Quan, Y. Yang, X. Yang, X. Meng, J. Huang and K. Wang, *Analyst*, 2020, **145**, 1925–1932.
- 110 H. Wang, H. Wang, Q. Wu, M. Liang, X. Liu and F. Wang, *Chem. Sci.*, 2019, **10**, 9597–9604.
- 111 W. Dang, C. Tong, Y. Yang, Y. Liu, B. Liu, H. Zhou and W. Wang, *Analyst*, 2019, **144**, 1731–1740.
- 112 R. Li, Q. Liu, Y. Jin and B. Li, *Anal. Chim. Acta*, 2019, **1079**, 139–145.
- 113 H. Yang, Y. Liu, Y. Wan, Y. Dong, Q. He, M. R. Khan, R. Busquets, G. He, J. Zhang, R. Deng and Z. Zhao, *Sci. Total Environ.*, 2023, **863**, 160899.
- 114 H. Gao, X. Song, Q. Chen, R. Yuan and Y. Xiang, *Anal. Chim. Acta*, 2023, **1247**, 340902.
- 115 W. Pan, D. Yu, Y. Qin, W. Wu, Y. Lu, Z. Yuan and J. Zhou, *Talanta*, 2019, **201**, 358–363.
- 116 C. Yuan, J. Fang and W. Fu, *Anal. Chem.*, 2023, **95**, 8291–8298.
- 117 F. Chang, Y. Sun, D. Yang, W. Yang, Y. Sun, C. Liu and Z. Li, *Chem. Commun.*, 2019, **55**, 6934–6937.
- 118 F. Su, T. Li, X. He and Z. Li, *Analyst*, 2022, **147**, 5649–5654.
- 119 Y. Sun, Y. Sun, W. Tian, C. Liu, K. Gao and Z. Li, *Chem. Sci.*, 2018, **9**, 1344–1351.
- 120 Y. An, Z. Yu, D. Liu, L. Han, X. Zhang, X. Xin and C. Li, *Anal. Bioanal. Chem.*, 2023, **415**, 2271–2280.
- 121 Q. Lin, Y. Cao, G. Han, W. Sun, W. Weng, H. Chen, H. Wang and J. Kong, *Anal. Chem.*, 2023, **95**, 13401–13406.
- 122 H. Zhang, L. J. Wang, L. Wang, H. Chen, X. Chen and C. Y. Zhang, *J. Mater. Chem. B*, 2019, **7**, 157–162.
- 123 Y. Zhang, Q. N. Li, D. X. Xiang, K. Zhou, Q. Xu and C. Y. Zhang, *Chem. Commun.*, 2020, **56**, 8952–8955.
- 124 W. Chen, H. Zhang, Y. Zhang, M. Hui, H. Chen, C. Ren, D. Di and H. Zhang, *Anal. Chim. Acta*, 2023, **1263**, 341275.
- 125 Y. P. Zhang, Y. X. Cui, X. Y. Li, Y. C. Du, A. N. Tang and D. M. Kong, *Chem. Commun.*, 2019, **55**, 7611–7614.
- 126 X. R. Cheng, F. Wang, C. Y. Liu, J. Li, C. Shan, K. Wang, Y. Wang, P. F. Li and X. M. Li, *Anal. Bioanal. Chem.*, 2022, **414**, 6139–6147.
- 127 D. Mao, T. Chen, H. Chen, M. Zhou, X. Zhai, G. Chen and X. Zhu, *Analyst*, 2019, **144**, 4060–4065.
- 128 Q. Yan, Q. Duan, Y. Huang, J. Guo, L. Zhong, H. Wang and G. Yi, *RSC Adv.*, 2019, **9**, 41305–41310.
- 129 H. Y. Kim, J. Song and H. G. Park, *Biosens. Bioelectron.*, 2021, **178**, 113048.
- 130 M. N. Emaus and J. L. Anderson, *Anal. Chim. Acta*, 2021, **1181**, 338900.
- 131 G. Han, D. Li, Q. Lin, J. Yi, Q. Lyu, Q. Ma and L. Qiao, *Chin. Chem. Lett.*, 2023, **34**, 107421.
- 132 J. Qian, Q. Zhang, M. Liu, Y. Wang and M. Lu, *Biosens. Bioelectron.*, 2022, **196**, 113707.
- 133 L. Zhang, H. Jiang, Z. Zhu, J. Liu and B. Li, *Talanta*, 2022, **243**, 123388.
- 134 Y. Zhao, F. Chen, Q. Li, L. Wang and C. Fan, *Chem. Rev.*, 2015, **115**, 12491–12545.
- 135 X. Cao, C. Chen and Q. Zhu, *Talanta*, 2023, **253**, 123977.
- 136 J. Ye, M. Xu, X. Tian, S. Cai and S. Zeng, *J. Pharm. Anal.*, 2019, **9**, 217–226.
- 137 X. Y. Hu, Z. Song, Z. W. Yang, J. J. Li, J. Liu and H. S. Wang, *Analyst*, 2022, **147**, 2615–2632.
- 138 C. Liu, C. Chen, S. Li, H. Dong, W. Dai, T. Xu, Y. Liu, F. Yang and X. Zhang, *Anal. Chem.*, 2018, **90**, 10591–10599.

